

MCMC analysis of WMAP3 and SDSS data points to broken symmetry inflaton potentials and provides a lower bound on the tensor to scalar ratio.

C. Destri^{(a),*} H. J. de Vega^{(b,c),†} and N. G. Sanchez^{(c)‡}

^(a) *Dipartimento di Fisica G. Occhialini, Università Milano-Bicocca Piazza della Scienza 3, 20126 Milano and INFN, sezione di Milano, via Celoria 16, Milano Italia*

^(b) *LPTHE, Laboratoire Associé au CNRS UMR 7589, Université Pierre et Marie Curie (Paris VI) et Denis Diderot (Paris VII), Tour 24, 5 ème. étage, 4, Place Jussieu, 75252 Paris, Cedex 05, France.*

^(c) *Observatoire de Paris, LERMA, Laboratoire Associé au CNRS UMR 8112, 61, Avenue de l'Observatoire, 75014 Paris, France.*

(Dated: August 15, 2018)

We perform a MCMC (Monte Carlo Markov Chains) analysis of the available CMB and LSS data (including the three years WMAP data) with single field slow-roll new inflation and chaotic inflation models. We do this within our approach to inflation as an effective field theory in the Ginsburg-Landau spirit with fourth degree trinomial potentials in the inflaton field ϕ . We derive explicit formulae and study in detail the spectral index n_s of the adiabatic fluctuations, the ratio r of tensor to scalar fluctuations and the running index $dn_s/d\ln k$. We use these analytic formulas as hard constraints on n_s and r in the MCMC analysis. Our analysis differs in this **crucial** aspect from previous MCMC studies in the literature involving the WMAP3 data. Our results are as follow: (i) The data strongly indicate the **breaking** (whether spontaneous or explicit) of the $\phi \rightarrow -\phi$ symmetry of the inflaton potentials both for new and for chaotic inflation. (ii) Trinomial new inflation naturally satisfies this requirement and provides an excellent fit to the data. (iii) Trinomial chaotic inflation produces the best fit in a very narrow corner of the parameter space. (iv) The chaotic symmetric trinomial potential is almost certainly **ruled out** (at 95%CL). In trinomial chaotic inflation the MCMC runs go towards a potential in the *boundary* of the parameter space and which resembles a spontaneously symmetry broken potential of new inflation. (v) The above results and further physical analysis here lead us to conclude that **new inflation** gives the best description of the data. (vi) We find a lower bound for r within trinomial new inflation potentials: $r > 0.016$ (95% CL) and $r > 0.049$ (68% CL). (vii) The preferred new inflation trinomial potential is a double well, even function of the field with a moderate quartic coupling yielding as most probable values: $n_s \simeq 0.958$, $r \simeq 0.055$. This value for r is within reach of forthcoming CMB observations.

Contents

I. Introduction and Results	2
II. The Inflaton Potential and the $1/N$ Slow Roll Expansion	5
III. Trinomial Chaotic Inflation: Spectral index, amplitude ratio, running index and limiting cases	8
A. The small asymmetry regime: $-1 < h \leq 0$.	9
B. The flat potential limit $h \rightarrow -1^+$	10
C. The singular limit $z = 1$ and then $h \rightarrow -1^+$ yields the Harrison-Zeldovich spectrum	11
D. The high asymmetry $h < -1$ regime.	13
IV. Trinomial New Inflation: Spectral index, amplitude ratio, running index and limiting cases	14
A. The shallow limit (weak coupling) $y \rightarrow 0$	16
B. The steep limit (strong coupling) $y \rightarrow \infty$	17
C. The extremely asymmetric limit $ h \rightarrow \infty$	17
D. Regions of n_s and r covered by New Inflation and by Chaotic Inflation.	18
V. Monte Carlo Markov Chains and data analysis with the trinomial inflation models	18

*Electronic address: Claudio.Destri@mib.infn.it

†Electronic address: devega@lpthe.jussieu.fr

‡Electronic address: Norma.Sanchez@obspm.fr

A. MCMC results for new inflation.	20
B. MCMC results for chaotic inflation.	22
C. Conclusions.	23
References	24

I. INTRODUCTION AND RESULTS

Inflation was introduced to solve several outstanding problems of the standard Big Bang model [1] and has now become an important part of the standard cosmology. At the same time, it provides a natural mechanism for the generation of scalar density fluctuations that seed large scale structure, thus explaining the origin of the temperature anisotropies in the cosmic microwave background (CMB), as well as that of tensor perturbations (primordial gravitational waves) [2, 3, 4].

A distinct aspect of inflationary perturbations is that these are generated by quantum fluctuations of the scalar field(s) that drive inflation. After their wavelength becomes larger than the Hubble radius, these fluctuations are amplified and grow, becoming classical and decoupling from causal microphysical processes. Upon re-entering the horizon, during the matter era, these classical perturbations seed the inhomogeneities which generate structure upon gravitational collapse [2, 3]. A great diversity of inflationary models predict fairly generic features: a gaussian, nearly scale invariant spectrum of (mostly) adiabatic scalar and tensor primordial fluctuations, making the inflationary paradigm fairly robust. The gaussian, adiabatic and nearly scale invariant spectrum of primordial fluctuations provide an excellent fit to the highly precise wealth of data provided by the Wilkinson Microwave Anisotropy Probe (WMAP)[5, 6]. Perhaps the most striking validation of inflation as a mechanism for generating *superhorizon* ('acausal') fluctuations is the anticorrelation peak in the temperature-polarization (TE) angular power spectrum at $l \sim 150$ corresponding to superhorizon scales [5]. The confirmation of many of the robust predictions of inflation by current high precision observations places inflationary cosmology on solid grounds.

Amongst the wide variety of inflationary scenarios, single field slow roll models provide an appealing, simple and fairly generic description of inflation. Its simplest implementation is based on a scalar field (the inflaton) whose homogeneous expectation value drives the dynamics of the scale factor, plus small quantum fluctuations. The inflaton potential is fairly flat during inflation. This flatness not only leads to a slowly varying Hubble parameter, hence ensuring a sufficient number of e-folds, but also provides an explanation for the gaussianity of the fluctuations as well as for the (almost) scale invariance of their power spectrum. A flat potential precludes large non-linearities in the dynamics of the *fluctuations* of the scalar field.

The current WMAP data seem to validate the simpler one-field slow roll scenario [5, 6]. Furthermore, because the potential is flat the scalar field is almost **massless**, and modes cross the horizon with an amplitude proportional to the Hubble parameter. This fact combined with a slowly varying Hubble parameter yields an almost scale invariant primordial power spectrum. The slow-roll approximation has been recently cast as a $1/N$ expansion [7], where $N \sim 50$ is the number of e-folds before the end of inflation when modes of cosmological relevance today first crossed the Hubble radius.

The observational progress permits to start to discriminate among different inflationary models, placing stringent constraints on them. The upper bound on the ratio r of tensor to scalar fluctuations obtained by WMAP [5, 6] **necessarily** implies the presence of a **mass term** in the single field inflaton potential and therefore rules out the massless monomial ϕ^4 potential [6, 7]. Hence, as minimal single field model, one should consider a sufficiently general quartic polynomial, that is the trinomial potential.

Besides its simplicity, the trinomial potential is a physically well motivated potential for inflation in the context of the Ginsburg-Landau approach to effective field theories (see for example ref.[10]). This potential is rich enough to describe the physics of inflation and accurately reproduce the WMAP data [5, 6].

The slow-roll expansion plus the WMAP data constraints the inflaton potential to have the form [7]

$$V(\phi) = N M^4 w(\chi) , \quad (1.1)$$

where ϕ is the inflaton field, χ is a dimensionless, slowly varying field

$$\chi \equiv \frac{\phi}{\sqrt{N} M_{Pl}} , \quad (1.2)$$

$w(\chi) \sim \mathcal{O}(1)$ and M is the energy scale of inflation which is determined by the amplitude of the scalar adiabatic fluctuations [5] to be

$$M \sim 0.00319 M_{Pl} = 0.77 \times 10^{16} \text{ GeV} . \quad (1.3)$$

Following the spirit of the Ginsburg-Landau theory of phase transitions, the simplest choice is a quartic trinomial for the inflaton potential [7, 8, 9]:

$$w(\chi) = w_0 \pm \frac{1}{2} \chi^2 + \frac{h}{3} \sqrt{\frac{y}{2}} \chi^3 + \frac{y}{32} \chi^4 , \quad (1.4)$$

where the coefficients w_0 , h and y are dimensionless and of order one and the signs \pm correspond to large field and small field inflation, respectively (namely, chaotic inflation and new inflation, respectively). h describes how asymmetric is the potential, y is the dimensionless quartic coupling.

Inserting eq.(1.4) in eq.(1.1) yields,

$$V(\phi) = V_0 \pm \frac{m^2}{2} \phi^2 + \frac{m g}{3} \phi^3 + \frac{\lambda}{4} \phi^4 , \quad (1.5)$$

where the mass m^2 and the couplings g and λ are given by the following see-saw-like relations,

$$m = \frac{M^2}{M_{Pl}} , \quad g = h \sqrt{\frac{y}{2 N}} \left(\frac{M}{M_{Pl}} \right)^2 , \quad \lambda = \frac{y}{8 N} \left(\frac{M}{M_{Pl}} \right)^4 , \quad V_0 = N M^4 w_0 . \quad (1.6)$$

Notice that $y \sim \mathcal{O}(1) \sim h$ guarantee that $g \sim \mathcal{O}(10^{-6})$ and $\lambda \sim \mathcal{O}(10^{-12})$ **without** any fine tuning as stressed in ref. [7]. That is, the smallness of the couplings here is not a consequence of fine tuning but follow directly from the form of the inflaton potential eq.(1.1) and the amplitude of the scalar fluctuations that fixes M [7].

During inflation the inflaton field χ slowly runs from its initial value till its final value χ_{end} at the absolute minima of the potential $w(\chi)$. We have $\chi_{end} = 0$ for chaotic inflation while χ_{end} turns to be a function of the coupling y and the asymmetry h for new inflation. Inflation ends after a *finite* number of e-folds provided

$$w(\chi_{end}) = w'(\chi_{end}) = 0$$

Enforcing this condition in the inflationary potential eq.(1.4) determines the constant w_0 . We have $w_0 = 0$ for chaotic inflation while w_0 turns to be a function of the coupling y and the asymmetry h for new inflation. χ can vary in the interval $(0, \infty)$ for chaotic inflation while χ is in the interval $(0, \chi_{end})$ for new inflation.

We derive explicit formulae and study in detail the spectral index n_s of the adiabatic fluctuations, the ratio r of tensor to scalar fluctuations and the running index $dn_s/d \ln k$ both for trinomial chaotic inflation and trinomial new inflation.

The small coupling limit $y \rightarrow 0$ of eqs.(1.4)-(1.5) corresponds to the quadratic monomial potential while the strong coupling limit $y \rightarrow \infty$ yields in chaotic inflation the massless quartic monomial potential. The extreme asymmetric limit $|h| \rightarrow \infty$ yields a massive model without quadratic term. In such a limit the product $|h| M^2$ must be kept fixed since it is determined by the amplitude of the scalar fluctuations.

In this paper we perform Monte Carlo Markov Chains (MCMC) analysis of the commonly available CMB and Large Scale Structure (LSS) data. For CMB we considered the three years WMAP data, which provide the dominating contribution, and also small scale data (ACBAR, CBI2, BOOMERANG03). For LSS we considered SDSS (Sloan Digital Sky Survey) [11]. We used the CosmoMC program [12] within the effective field theory of inflation. We used a large collection of parallel chains with a total number of samples close to five million. For chaotic and new inflation we imposed as a hard constraint that the spectral index n_s of the adiabatic fluctuations and the ratio r are given by the analytic formulas at order $1/N$ we derived for the trinomial inflaton potential. Our analysis differs in this **crucial** aspect from previous MCMC studies involving the WMAP3 data set [11]. As natural within inflation, we also included the inflationary consistency relation $n_T = -r/8$ on the tensor spectral index. This constraint is in any case practically negligible. The details of the MCMC analysis are explained in Section V.

Our approach is different to the inflationary flow equations [14] where the inflaton potential **changes** (that is, **the model changes**) as the flow goes on. We work with a **given** potential within the Ginsburg-Landau (GL) spirit, that is the trinomial potential. We investigate the physics of the chosen potential in the parameter space driven by the data through the Monte Carlo Markov Chains. In our work, n_s and r are computed analytically to order $1/N$ for the

trinomial potentials [eqs.(3.6)-(3.8) and (4.6)-(4.8)]. Since $N \sim 50$, higher order corrections in $1/N$ are irrelevant and can be safely neglected. As shown in ref. [7], the slow roll expansion is in fact a systematic expansion in $1/N$.

We allowed seven cosmological parameters to vary in our MCMC runs: the scalar spectral index n_s , the tensor-scalar ratio r , the baryonic matter fraction ω_b , the dark matter fraction ω_c , the optical depth τ , the ratio of the (approximate) sound horizon to the angular diameter distance θ and the primordial superhorizon power in the curvature perturbation at 0.05 Mpc^{-1} , A_s . We allowed the same seven parameters to vary in the MCMC runs for chaotic and new inflation.

In the case of new inflation, since the characteristic banana-shaped allowed region in the (n_s, r) plane [fig. 2] is quite narrow and non-trivial, it is convenient to use the two independent variables $z \equiv \frac{y}{8} \chi^2$ and h in trinomial inflationary setup as MC parameters. That is, we used the analytic expressions we found at order $1/N$, to express n_s and r in terms of z and h .

Concerning priors, we kept the same, standard ones, of the $\Lambda\text{CDM}+r$ model for the first five parameters (ω_b , ω_c , τ , θ and A_s), while we considered all the possibilities for z and h .

In the case of chaotic inflation we kept n_s and r as MC parameters, imposing as hard priors that they lay in the region described by chaotic inflation [fig. 2]. This is technically convenient, since this region covers the major part of the probability support of n_s and r in the $\Lambda\text{CDM}+r$ and the parametrization eqs.(3.6)-(3.8) in terms of the parameters z and h becomes quite singular in the limit $h \rightarrow -1$. This is indeed the limit which allows to cover the region of highest likelihood. The priors on the other parameters were the same of the $\Lambda\text{CDM}+r$ model and of new inflation.

We did not marginalize over the SZ amplitude, and we did not include non-linear effects in the evolution of the matter spectrum. The relative corrections are in any case not significant [5], especially in the present context.

In all our MCMC runs we keep fixed the number of e-folds N since horizon exit till the end of inflation. The reason is that the main physics that determines the value of N is **not** contained in the available data but involves the reheating era. Therefore, it is **not** reliable to fit N solely to the CMB and LSS data. The precise value of N is certainly near $N = 50$ [14, 15]. We take here the value $N = 50$ as a reference baseline value for numerical analysis, but from the explicit expressions obtained in the slow roll $1/N$ expansion we see that both $n_s - 1$ and r scale as $1/N$. Therefore, varying N produces a scale transformation in the $(n_s - 1, r)$ plane, thus displacing the black and red curves in fig. 2 towards up and left or towards down and right. This produces however small quantitative changes in our bounds for r as well as in the most probable values for r and n_s . MCMC simulations with variable N and imposing the trinomial new inflation potential yielded $N \sim 50$ as the most probable value.

We plot in fig. 2 r vs. n_s both for chaotic and new inflation for fixed values of the asymmetry h and the coupling y varying along the curves. We see that the regions of the trinomial new inflation and chaotic inflation are **complementary** in the (n_s, r) plane. The red curves are those of chaotic inflation, while black curves are for new inflation. The leftmost black line corresponds to new inflation with a symmetric potential $h = 0$. The rightmost black line describes the case of new inflation with an extreme asymmetric potential $|h| \gg 1$. This last line is the border of the region on the right described by chaotic inflation. Although chaotic inflation covers a much wider area than new inflation, this wide area is only a small corner of the parameter space (field $z \equiv \frac{y}{8} \chi^2$, asymmetry h) as shown by fig. 9.

For the trinomial **new inflation** model we find a **lower bound** on r :

$$r > 0.016 \quad (95\% \text{ CL}) \quad , \quad r > 0.049 \quad (68\% \text{ CL}) \quad (\text{new inflation}) . \quad (1.7)$$

while for n_s we find:

$$n_s > 0.945 \quad (95\% \text{ CL}) \quad (\text{new inflation}) .$$

The most probable values are (see fig. 6),

$$n_s \simeq 0.956 \quad , \quad r \simeq 0.055 \quad (\text{new inflation}) . \quad (1.8)$$

For trinomial new inflation there exists the theoretical upper limits: $n_s \leq 0.9615\dots$, $r \leq 0.16$ [9]. Thus, the *most probable value* of n_s for trinomial new inflation eq.(1.8) is very close to its *theoretical limiting value*, and that of r is not too far from it (see also fig. 6).

The probability distribution for the asymmetry parameter h is peaked at $h = 0$ with

$$|h| < 4.92 \text{ with } 95\% \text{ CL} \quad \text{new inflation} .$$

That is, we find that the most probable trinomial new inflation potential is symmetric and has a moderate nonlinearity with the quartic coupling $y \simeq 2$ for $h \simeq 0$. This is the following potential:

$$w(\chi) = \frac{y}{32} \left(\chi^2 - \frac{8}{y} \right)^2 . \quad (1.9)$$

The $\chi \rightarrow -\chi$ symmetry is here broken since the absolute minimum of the potential is at $\chi \neq 0$.

For trinomial **chaotic inflation**, the chaotic symmetric trinomial potential $h = 0$ is almost certainly **ruled out** since $h < -0.7$ at 95 % confidence level (see fig. 9).

We see the maximum probability for strong asymmetry $h < -0.95$ and significant nonlinearity $4.207 \dots < y < +\infty$. That is, in chaotic inflation *all three* terms in the trinomial potential $w(\chi)$ **do** contribute.

We have not introduced the running of the spectral index $dn_s/d \ln k$ in our MCMC fits since the running must be very small of the order $\mathcal{O}(N^{-2}) \sim 0.001$ in slow-roll and for generic potentials [7]. We find that adding the new parameter $dn_s/d \ln k$ to the MCMC analysis make negligible changes on the fit of n_s and r . All this suggests that the present data are **not** yet precise enough to allow a determination of $dn_s/d \ln k$.

In summary, the data favour the breaking of the $\chi \rightarrow -\chi$ symmetry both for new and for chaotic inflation.

Trinomial chaotic inflation produces its best fit to the data in a **very narrow** corner of the parameter space.

The potential in chaotic inflation has a single minimum. But this minimum for the best fit potential happens to be in the boundary of the parameter space, precisely where the asymmetry of the potential is so large that arises an extra minimum to the potential. That is, the data are begging the potential to be a double well (that is, a new inflation potential). The MCMC runs go towards a potential in the *boundary* of the parameter space and maximal symmetry breaking. This limiting potential exhibits an inflexion point and a significative nonlinearity. This strongly suggest that the true potential may be outside the parameter space of chaotic inflation. On the contrary, starting with a double well, that is new inflation, the data are perfectly well fitted with small or even zero asymmetry.

In chaotic inflation, the MCMC minimization leads to a large nonlinearity (from the higher order cubic and quartic terms), making chaotic inflation not stable under higher order terms in the potential. Chaotic inflation thus results contrary to the Ginsburg-Landau spirit in which higher order terms of the potential must be smaller and smaller giving irrelevant corrections.

On the contrary, new inflation results perfectly well fitted by the data with very small or zero cubic non-linearity, and thus new inflation is stable under higher order terms of the potential, which is perfectly well within the Ginsburg-Landau spirit.

Indeed, one can fit the WMAP+LSS data both with trinomial new inflation as well as with trinomial chaotic inflation. However, the trinomial potential that gives the best fit for chaotic inflation is theoretically **undesirable** for the reasons explained above. Therefore, trinomial new inflation is the **best model** that describes the data. This implies that we **do have** a lower bound on r as given by eq.(1.7). Moreover, the best fit is obtained with the double well inflation potential eq.(1.9) yielding the values in eq.(1.8) for n_s and r .

This paper is organized as follows: in section II we discuss the slow-roll approach as the $1/N$ expansion. In sections III and IV we present the trinomial chaotic inflation and the new trinomial inflation, respectively, displaying the analytic formulas for the spectral index n_s of the adiabatic fluctuations, the ratio r of tensor to scalar fluctuations and the running index $dn_s/d \ln k$. In section V we explain our MCMC analysis, we present our MCMC results for new and chaotic trinomial inflation and we state our conclusions.

II. THE INFLATON POTENTIAL AND THE $1/N$ SLOW ROLL EXPANSION

The description of cosmological inflation is based on an isotropic and homogeneous geometry, which assuming flat spatial sections is determined by the invariant distance

$$ds^2 = dt^2 - a^2(t) d\vec{x}^2 . \quad (2.1)$$

The scale factor obeys the Friedman equation

$$H^2(t) = \frac{\rho(t)}{3 M_{Pl}^2} , \quad \text{where} \quad H(t) \equiv \frac{1}{a(t)} \frac{da}{dt} , \quad (2.2)$$

where $\rho(t)$ is the total energy density and $M_{Pl} = 1/\sqrt{8\pi G} = 2.4 \times 10^{18}$ GeV.

In single field inflation the energy density is dominated by a homogeneous scalar *condensate*, the inflaton, whose dynamics is described by an *effective* Lagrangian

$$\mathcal{L} = a^3(t) \left[\frac{\dot{\phi}^2}{2} - \frac{(\nabla\phi)^2}{2a^2(t)} - V(\phi) \right]. \quad (2.3)$$

The inflaton potential $V(\phi)$ is a slowly varying function of ϕ in order to permit a slow-roll solution for the inflaton field $\phi(t)$. We showed in ref.[7] that combining the slow roll expansion with the WMAP data yields an inflaton potential of the form

$$V(\phi) = N M^4 w(\chi), \quad (2.4)$$

where χ is a dimensionless, slowly varying field

$$\chi = \frac{\phi}{\sqrt{N} M_{Pl}}, \quad (2.5)$$

$w(\chi) \sim \mathcal{O}(1)$, $N \sim 50$ is the number of e-folds since the cosmologically relevant modes exited the horizon till the end of inflation and M is the energy scale of inflation

The dynamics of the rescaled field χ exhibits the slow time evolution in terms of the *stretched* dimensionless time variable,

$$\tau = \frac{t M^2}{M_{Pl} \sqrt{N}}, \quad \mathcal{H} \equiv \frac{H}{\sqrt{N} m} = \mathcal{O}(1). \quad (2.6)$$

The rescaled variables χ and τ change slowly with time. A large change in the field amplitude ϕ results in a small change in the χ amplitude, a change in $\phi \sim M_{Pl}$ results in a χ change $\sim 1/\sqrt{N}$. The form of the potential, eq.(2.4) and the rescaled dimensionless inflaton field eq.(2.5) and time variable τ make **manifest** the slow-roll expansion as a consistent systematic expansion in powers of $1/N$ [7].

The inflaton mass around the minimum is given by a see-saw formula

$$m = \frac{M^2}{M_{Pl}} \sim 2.45 \times 10^{13} \text{ GeV}.$$

The Hubble parameter when the cosmologically relevant modes exit the horizon is given by

$$H = \sqrt{N} m \mathcal{H} \sim 1.0 \times 10^{14} \text{ GeV} = 4.1 m,$$

where we used that $\mathcal{H} \sim 1$. As a result, $m \ll M$ and $H \ll M_{Pl}$.

A Ginsburg-Landau realization of the inflationary potential that fits the amplitude of the CMB anisotropy remarkably well, reveals that the Hubble parameter, the inflaton mass and non-linear couplings are see-saw-like, namely powers of the ratio M/M_{Pl} multiplied by further powers of $1/N$. Therefore, the smallness of the couplings is not a result of fine tuning but a **natural** consequence of the form of the potential and the validity of the effective field theory description and slow roll. The quantum expansion in loops is therefore a double expansion on $(H/M_{Pl})^2$ and $1/N$. Notice that graviton corrections are also at least of order $(H/M_{Pl})^2$ because the amplitude of tensor modes is of order H/M_{Pl} . We showed that the form of the potential which fits the WMAP data and is consistent with slow roll eqs.(2.4)-(2.5) implies the small values for the inflaton self-couplings [7].

The equations of motion in terms of the dimensionless rescaled field χ and the slow time variable τ take the form,

$$\begin{aligned} \mathcal{H}^2(\tau) &= \frac{1}{3} \left[\frac{1}{2N} \left(\frac{d\chi}{d\tau} \right)^2 + w(\chi) \right], \\ \frac{1}{N} \frac{d^2\chi}{d\tau^2} + 3 \mathcal{H} \frac{d\chi}{d\tau} + w'(\chi) &= 0. \end{aligned} \quad (2.7)$$

The slow-roll approximation follows by neglecting the $\frac{1}{N}$ terms in eqs.(2.7). Both $w(\chi)$ and $\mathcal{H}(\tau)$ are of order N^0 for large N . Both equations make manifest the slow roll expansion as an expansion in $1/N$.

The number of e-folds $N[\chi]$ since the field χ exits the horizon till the end of inflation (where χ takes the value χ_{end}) can be computed in close form from eqs. (2.7) in the slow-roll approximation (neglecting $1/N$ corrections)

$$\frac{N[\chi]}{N} = - \int_{\chi}^{\chi_{end}} \frac{w(\chi)}{w'(\chi)} d\chi \leq 1. \quad (2.8)$$

Inflation ends after a finite number of efolds provided

$$w(\chi_{end}) = w'(\chi_{end}) = 0 \quad (2.9)$$

This condition will be enforced in the inflationary potentials.

The amplitude of adiabatic scalar perturbations is expressed as [3, 4, 5, 7]

$$|\Delta_{k\ ad}^{(S)}|^2 = \frac{N^2}{12\pi^2} \left(\frac{M}{M_{Pl}} \right)^4 \frac{w^3(\chi)}{w'^2(\chi)}. \quad (2.10)$$

The spectral index n_s , its running and the ratio of tensor to scalar fluctuations are expressed as

$$\begin{aligned} n_s - 1 &= -\frac{3}{N} \left[\frac{w'(\chi)}{w(\chi)} \right]^2 + \frac{2}{N} \frac{w''(\chi)}{w(\chi)}, \\ \frac{dn_s}{d \ln k} &= -\frac{2}{N^2} \frac{w'(\chi) w'''(\chi)}{w^2(\chi)} - \frac{6}{N^2} \frac{[w'(\chi)]^4}{w^4(\chi)} + \frac{8}{N^2} \frac{[w'(\chi)]^2 w''(\chi)}{w^3(\chi)}, \\ r &= \frac{8}{N} \left[\frac{w'(\chi)}{w(\chi)} \right]^2. \end{aligned} \quad (2.11)$$

In eqs.(2.8)-(2.11) the field χ is computed at horizon exiting. We choose $N[\chi] = N = 50$.

Since, $w(\chi)$ and $w'(\chi)$ are of order one, we find from eq.(2.10)

$$\left(\frac{M}{M_{Pl}} \right)^2 \sim \frac{2\sqrt{3}\pi}{N} |\Delta_{k\ ad}^{(S)}| \simeq 1.02 \times 10^{-5}. \quad (2.12)$$

where we used $N \simeq 50$ and the WMAP value for $|\Delta_{k\ ad}^{(S)}| = (4.67 \pm 0.27) \times 10^{-5}$ [5]. This fixes the scale of inflation to be

$$M \simeq 3.19 \times 10^{-3} M_{Pl} \simeq 0.77 \times 10^{16} \text{ GeV}.$$

This value *pinpoints the scale of the potential* during inflation to be at the GUT scale suggesting a deep connection between inflation and the physics at the GUT scale in cosmological space-time.

We see that $|n_s - 1|$ as well as the ratio r turn out to be of order $1/N$. This nearly scale invariance is a natural property of inflation which is described by a quasi-de Sitter space-time geometry. This can be understood intuitively as follows: the geometry of the universe is scale invariant during de Sitter stage since the metric takes in conformal time the form

$$ds^2 = \frac{1}{(H\eta)^2} [(d\eta)^2 - (d\vec{x})^2].$$

Therefore, the primordial power generated is scale invariant except for the fact that inflation is not eternal and lasts for N efolds. Hence, the primordial spectrum is scale invariant up to $1/N$ corrections. The Harrison-Zeldovich values $n_s = 1$, $r = 0$ and $dn_s/d \ln k = 0$ correspond to a critical point as discussed in ref.[7]. This gaussian fixed point is **not** the inflationary model that reproduces the data but the inflation model hovers around it in the renormalization group sense with an almost scale invariant spectrum of scalar fluctuations during the slow roll stage.

We analyze in the subsequent sections chaotic inflation and new inflation in its simple physical realizations within the Ginzburg-Landau approach (the trinomial potential)[7, 8, 9]. We perform with these models Monte Carlo Markov chains analysis of the three years WMAP data and LSS data.

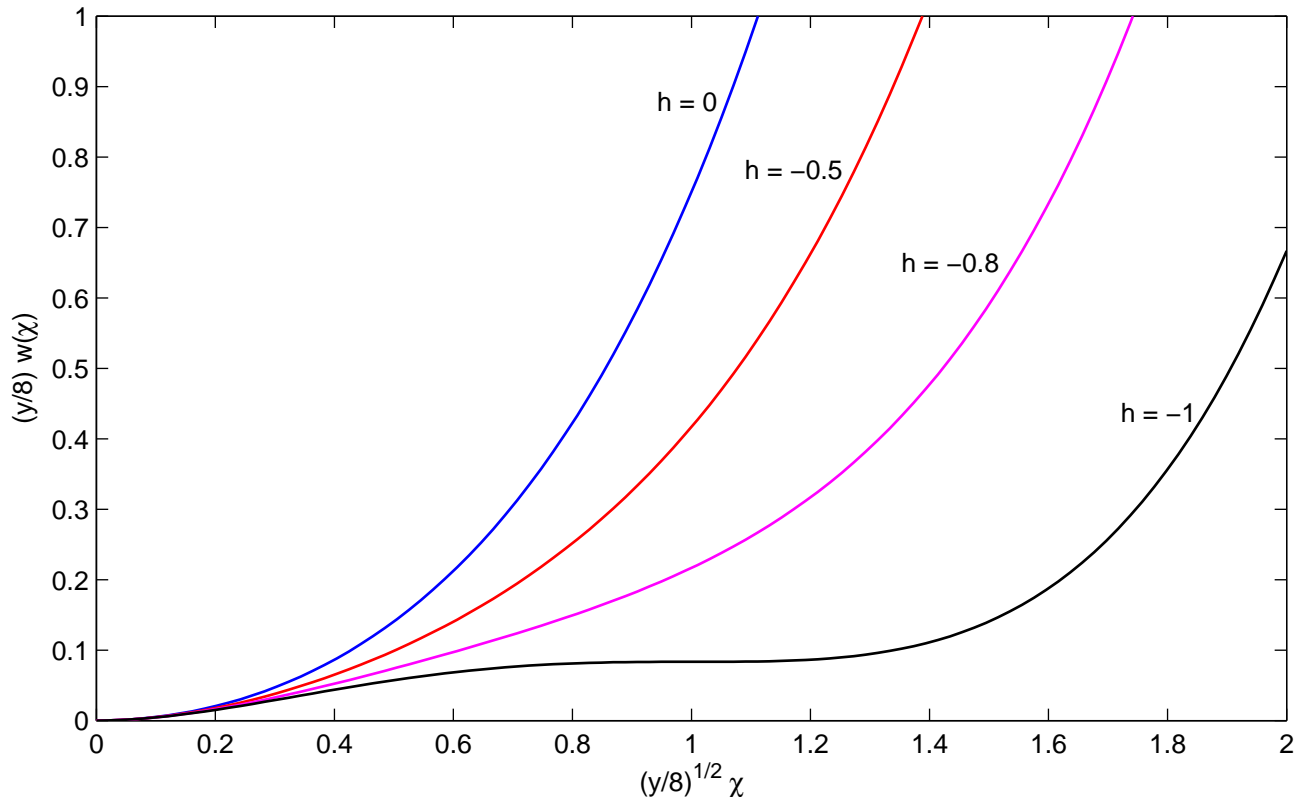


FIG. 1: Trinomial Chaotic Inflation. We plot here the chaotic inflation trinomial potential [eq.(3.2) with positive quadratic term] $\frac{y}{8} w(\chi)$ vs. the field variable $\sqrt{z} = \sqrt{y/8} \chi$ for different values of the asymmetry parameter h , namely, $h = 0, -0.5, -0.8$ and -1 . Notice the inflection point at $\sqrt{z} = 1$ when $h = -1$.

III. TRINOMIAL CHAOTIC INFLATION: SPECTRAL INDEX, AMPLITUDE RATIO, RUNNING INDEX AND LIMITING CASES

We consider now the trinomial potential with unbroken symmetry investigated in ref.[8]:

$$V(\phi) = \frac{m^2}{2} \phi^2 + \frac{m g}{3} \phi^3 + \frac{\lambda}{4} \phi^4, \quad (3.1)$$

where $m^2 > 0$ and g and λ are dimensionless couplings.

The corresponding dimensionless potential $w(\chi)$ eqs.(1.1)-(1.2) takes the form

$$w(\chi) = \frac{1}{2} \chi^2 + \frac{h}{3} \sqrt{\frac{y}{2}} \chi^3 + \frac{y}{32} \chi^4, \quad (3.2)$$

where the quartic coupling y is dimensionless as well as the asymmetry parameter h . The couplings in eq.(3.1) and eq.(3.2) are related by eq.(1.6).

Chaotic inflation is obtained by choosing the initial field χ in the interval $(0, +\infty)$. The inflaton χ slowly rolls down the slope of the potential from its initial value till the absolute minimum of the potential at the origin.

Computing the number of e-folds from eq.(2.8), we find the field χ at horizon crossing related to the couplings y and h . Without loss of generality, we choose $h < 0$ and shall work with positive fields χ .

The potential eq.(3.2) has extrema at $\chi = 0$ and χ_{\pm} given by,

$$\chi_{\pm} = \sqrt{\frac{8}{y}} [-h \pm i \Delta] \quad , \quad \Delta \equiv \sqrt{1 - h^2}. \quad (3.3)$$

That is, for $|h| < 1$, $w(\chi)$ has only one real extremum at $\chi = 0$ while for $|h| \geq 1$, $w(\chi)$ has three real extrema. There is always a minimum at $\chi = 0$ since $w''(0) = 1$. At the non-zero extrema we have

$$w''(\chi_{\pm}) = -2 \Delta (\Delta \pm i h) .$$

We have for $|h| > 1$,

$$\chi_{\pm} = \sqrt{\frac{8}{y}} \left[-h \pm \sqrt{h^2 - 1} \right], \quad \text{and} \quad w''(\chi_{\pm}) = 2\sqrt{h^2 - 1} \left(\sqrt{h^2 - 1} \mp h \right).$$

Hence, for any $h < -1$, we have $w''(\chi_+) > 0$ while $w''(\chi_-) < 0$. Notice that $\chi_{\pm} > 0$ for $h < -1$.

Therefore, we have chaotic inflation for positive field χ in the regime $|h| < 1$ using the inflaton potential eq.(3.2).

We can also have chaotic inflation with the potential eq.(3.2) for negative field if $h > 3/\sqrt{8}$, but for $|h| > 3/\sqrt{8}$ the absolute minimum is no more at $\chi = 0$ but at χ_+ . Since $w(\chi_+) < 0$ for $|h| > 3/\sqrt{8}$ we have to subtract in this case the value $w(\chi_+)$ from $w(\chi)$ in order to enforce eq.(2.9).

We consider in subsections III A, III B and III C the regime $-1 < h \leq 0$, $\chi \geq 0$. The case $h < -1$ is analyzed in subsection III D.

A. The small asymmetry regime: $-1 < h \leq 0$.

In chaotic inflation the inflaton field slowly rolls down the slope of the potential from its initial value till the absolute minimum of the potential at $\chi = 0$.

It is convenient to define the field variable z by:

$$z \equiv \frac{y}{8} \chi^2. \quad (3.4)$$

In terms of z the chaotic trinomial potential takes the form

$$w(\chi) = \frac{4}{y} z \left(1 + \frac{4}{3} h \sqrt{z} + \frac{1}{2} z \right).$$

When $z \lesssim 1$ we are in the quadratic regime where $w(\chi)$ is approximated by the χ^2 term. For $z \gtrsim 1$ we go to the non-linear regime in z and all three terms in $w(\chi)$ are of the same order of magnitude.

In fig. 1, we plot $\frac{y}{8} w(\chi)$ as a function of \sqrt{z} for several values of $h \geq -1$. We see that the potential becomes flatter as h decreases. For $h = -1$, both $w'(\chi)$ and $w''(\chi)$ vanish at $\sqrt{z} = 1$. The case $h = -1$ is singular since the inflaton gets stuck an infinite amount of time at the point $\sqrt{z} = 1$.

By inserting eq.(3.2) for $w(\chi)$ into eq.(2.8) for $N[\chi]$ and setting $N[\chi] = N$ we obtain the field χ or equivalently z , at horizon exit, in terms of the coupling y and the asymmetry parameter h ,

$$y = z + \frac{4}{3} h \sqrt{z} + \left(1 - \frac{4}{3} h^2 \right) \log(1 + 2h\sqrt{z} + z) - \frac{4h}{3\Delta} \left(\frac{5}{2} - 2h^2 \right) \left[\arctan\left(\frac{h + \sqrt{z}}{\Delta}\right) - \arctan\left(\frac{h}{\Delta}\right) \right] \quad (3.5)$$

This defines the field z as a monotonically increasing function of the coupling y for $0 < y$, $z < +\infty$. Recall that χ and z corresponds to the time of horizon exit.

We obtain from eqs.(2.10), (2.11) and (3.2) the spectral index, its running, the ratio r and the amplitude of adiabatic perturbations,

$$n_s = 1 - \frac{y}{2Nz} \left[3 \frac{(1 + 2h\sqrt{z} + z)^2}{\left(1 + \frac{4}{3}h\sqrt{z} + \frac{1}{2}z\right)^2} - \frac{1 + 4h\sqrt{z} + 3z}{1 + \frac{4}{3}h\sqrt{z} + \frac{1}{2}z} \right], \quad (3.6)$$

$$\begin{aligned} \frac{dn_s}{d \ln k} = & \frac{y^2}{2z^2 N^2} \left[-\frac{(1 + 2h\sqrt{z} + z)(h\sqrt{z} + \frac{3}{2}z)}{\left(1 + \frac{4}{3}h\sqrt{z} + \frac{1}{2}z\right)^2} - 3 \frac{(1 + 2h\sqrt{z} + z)^4}{\left(1 + \frac{4}{3}h\sqrt{z} + \frac{1}{2}z\right)^4} + \right. \\ & \left. + 2 \frac{(1 + 2h\sqrt{z} + z)^2 (1 + 4h\sqrt{z} + 3z)}{\left(1 + \frac{4}{3}h\sqrt{z} + \frac{1}{2}z\right)^3} \right], \quad (3.7) \end{aligned}$$

$$r = \frac{4y}{Nz} \frac{(1 + 2h\sqrt{z} + z)^2}{\left(1 + \frac{4}{3}h\sqrt{z} + \frac{1}{2}z\right)^2}, \quad (3.8)$$

$$|\Delta_{k ad}^{(S)}|^2 = \frac{2 N^2}{3 \pi^2} \left(\frac{M}{M_{Pl}} \right)^4 \frac{z^2 \left(1 + \frac{4}{3} h \sqrt{z} + \frac{1}{2} z \right)^3}{y^2 \left(1 + 2 h \sqrt{z} + z \right)^2}. \quad (3.9)$$

In chaotic inflation, the limit $z \rightarrow 0^+$ implies $y \rightarrow 0^+$ (shallow limit), we have in this limit:

$$\begin{aligned} y \stackrel{z \rightarrow 0^+}{\simeq} 2z + \mathcal{O}(z^{\frac{3}{2}}) \quad , \quad n_s \stackrel{y \rightarrow 0^+}{\simeq} 1 - \frac{2}{N}, \\ r \stackrel{y \rightarrow 0^+}{\simeq} \frac{8}{N} \quad , \quad |\Delta_{k ad}^{(S)}|^2 \stackrel{y \rightarrow 0^+}{\simeq} \frac{N^2}{6 \pi^2} \left(\frac{M}{M_{Pl}} \right)^4. \end{aligned} \quad (3.10)$$

The results in the $y \rightarrow 0^+$ limit are **independent** of the asymmetry h and coincide with those for the purely quadratic monomial potential $\frac{1}{2} \chi^2$.

In the limit $z \rightarrow +\infty$ which implies $y \rightarrow +\infty$ (steep limit), we have for fixed $h > -1$,

$$\begin{aligned} y \stackrel{z \rightarrow +\infty}{\simeq} z + \frac{4}{3} h \sqrt{z} + \left(1 - \frac{4}{3} h^2 \right) \log z + \mathcal{O}(1), \\ n_s \stackrel{y \rightarrow +\infty}{\simeq} 1 - \frac{3}{N} \left[1 + \frac{4}{3} \frac{h}{\sqrt{z}} + \left(1 - \frac{4}{3} h^2 \right) \frac{\log z}{z} + \mathcal{O}\left(\frac{1}{z}\right) \right], \\ r \stackrel{y \rightarrow +\infty}{\simeq} \frac{16}{N} \left[1 + \frac{4}{3} \frac{h}{\sqrt{z}} + \left(1 - \frac{4}{3} h^2 \right) \frac{\log z}{z} + \mathcal{O}\left(\frac{1}{z}\right) \right], \\ |\Delta_{k ad}^{(S)}|^2 \stackrel{y \rightarrow +\infty}{\simeq} \frac{N^2}{12 \pi^2} \left(\frac{M}{M_{Pl}} \right)^4 \frac{z}{\left[1 + \frac{4}{3} \frac{h}{\sqrt{z}} + \left(1 - \frac{4}{3} h^2 \right) \frac{\log z}{z} + \mathcal{O}\left(\frac{1}{z}\right) \right]^2}. \end{aligned} \quad (3.11)$$

For $h = 0$, n_s and r in the limit $y \rightarrow +\infty$ coincide with those of the purely quartic monomial potential $\frac{1}{2} \chi^4$:

$$n_s = 1 - \frac{3}{N} \quad , \quad r = \frac{16}{N}. \quad (3.12)$$

B. The flat potential limit $h \rightarrow -1^+$

We consider chaotic inflation in the regime $-1 < h \leq 0$, $\chi \geq 0$.

At $h = -1$ the potential eq.(3.2) exhibits an inflexion point at $\chi_0 \equiv \sqrt{\frac{8}{y}}$. Namely, $w'(\chi_0) = w''(\chi_0) = 0$ while $w(\chi_0) = 2/(3y) > 0$. That is, this happens at $z_0 = \frac{y}{8} \chi_0^2 = 1$.

Therefore, for $h > -1$ but very close to $h = -1$, the field evolution strongly slows down near the point $\chi = \chi_0$. This strong slow down shows up in the calculation of observables when the field χ at horizon crossing is $\chi > \chi_0$, namely, for $z > z_0 = 1$. For $\chi < \chi_0$, that is $z < 1$, the slow down of the field evolution will only appear if $z \simeq 1$. Therefore, the limit $h = -1$ is singular since the inflaton field gets trapped at the point $z = 1$.

Let us derive the $h \rightarrow -1^+$ limit of y , n_s and r from eqs.(3.5)-(3.9) in the regimes $z < 1$ and $z > 1$, respectively.

When $h \rightarrow -1^+$ we see from eq.(3.3) that $\Delta \rightarrow 0$ and the arguments of the two arctan in eq.(3.5) diverge. Hence, the arctan tends to $+\pi/2$ or $-\pi/2$. Depending on whether $z < 1$ or $z > 1$, the $\pi/2$'s terms cancel out or add, respectively. The special case $z = 1$ is investigated in the next subsection III C.

In the case $z < 1$ we get:

$$y = z - \frac{4}{3} \sqrt{z} - \frac{2}{3} \log(1 - \sqrt{z}) + \frac{2}{3} \frac{\sqrt{z}}{1 - \sqrt{z}} \quad , \quad h \rightarrow -1^+ \quad , \quad z < 1, \quad (3.13)$$

$$n_s = 1 - \frac{y}{2Nz} \left[3 \frac{(1 - \sqrt{z})^4}{\left(1 - \frac{4}{3} \sqrt{z} + \frac{1}{2} z \right)^2} - \frac{(1 - \sqrt{z})(1 - 3\sqrt{z})}{1 - \frac{4}{3} \sqrt{z} + \frac{1}{2} z} \right] \quad , \quad h \rightarrow -1^+ \quad , \quad z < 1, \quad (3.14)$$

$$r = \frac{4y}{Nz} \frac{(1 - \sqrt{z})^4}{\left(1 - \frac{4}{3} \sqrt{z} + \frac{1}{2} z \right)^2} \quad , \quad h \rightarrow -1^+ \quad , \quad z < 1,$$

$$|\Delta_{k\text{ ad}}^{(S)}|^2 = \frac{2N^2}{3\pi^2} \left(\frac{M}{M_{Pl}}\right)^4 \frac{z^2 \left(1 - \frac{4}{3}\sqrt{z} + \frac{1}{2}z\right)^3}{y^2 (1 - \sqrt{z})^4}. \quad (3.15)$$

In particular, in the regime $z \rightarrow 1^-$ we find,

$$\begin{aligned} n_s \stackrel{z \rightarrow 1^-}{\cong} 1 - \frac{4}{N}, \quad r \stackrel{z \rightarrow 1^-}{\cong} \frac{96}{N} (1 - \sqrt{z})^3 \rightarrow 0, \quad h \rightarrow -1^+, \\ y \stackrel{z \rightarrow 1^-}{\cong} \frac{2}{3} \frac{1}{1 - \sqrt{z}} \rightarrow \infty, \quad |\Delta_{k\text{ ad}}^{(S)}|^2 \stackrel{z \rightarrow 1^-}{\cong} \left(\frac{N}{8\pi} \frac{M^2}{M_{Pl}^2} y\right)^2. \end{aligned} \quad (3.16)$$

That is, in the limit $h \rightarrow -1^+$, $z \rightarrow 1^-$ the ratio r becomes **very small** while the spectral index takes the value $n_s = 0.92$. The ratio r tends to zero in the regime $z \rightarrow 1^-$, $\chi \rightarrow \chi_0 = \sqrt{\frac{8}{y}}$ because $w'(\chi_0) = 0$ and r is proportional to $w'^2(\chi)$ according to eq.(2.11).

The $z \rightarrow 1^-$ regime for $h \rightarrow -1^+$ is a strong coupling limit since $y \rightarrow +\infty$ as shown by eq.(3.16). In addition, eq.(3.16) shows that for large y one must keep the product $y M^2$ fixed since it is determined by the amplitude of the adiabatic perturbations. We see from eq.(3.16) that $\tilde{M} \equiv \sqrt{y} M$ becomes the energy scale of inflation in the $y \rightarrow \infty$ limit: from eq.(1.3), $\tilde{M} \sim 10^{16} \text{GeV}$ according to the observed value of $|\Delta_{k\text{ ad}}^{(S)}|/N$ displayed in eq.(2.12), while M and m vanish in the $y \rightarrow \infty$ limit

$$M = \frac{\tilde{M}}{\sqrt{y}} \stackrel{y \rightarrow \infty}{\cong} 0, \quad m = \frac{M^2}{M_{Pl}} = \frac{\tilde{M}^2}{y M_{Pl}} \stackrel{y \rightarrow \infty}{\cong} 0.$$

In fig. 2 we display r vs. n_s for fixed values of the asymmetry parameter h and the coupling y varying along the curves. The red curves correspond to chaotic inflation. In the bottom of fig. 2 we can see the curve for $h = -0.999$. The limiting curve for $h = -1$ (not drawn) will reach the point $n_s = 0.92$ and the bottom line $r = 0$ as described by eq.(3.16).

We see from fig. 2 that the regions of the trinomial new inflation and chaotic inflation are **complementary** in the (n_s, r) plane. New inflation describes the region of the (n_s, r) plane between the two black lines while chaotic inflation describes the whole plane to the right of the rightmost black line.

In the case $z > 1$, we get from eqs.(3.5)-(3.9),

$$\begin{aligned} y \stackrel{h \rightarrow -1^+}{\cong} \frac{\pi}{3} \sqrt{\frac{2}{h+1}} + \mathcal{O}([h+1]^0) \rightarrow +\infty, \quad z > 1, \\ n_s \stackrel{h \rightarrow -1^+}{\cong} 1 - \frac{\pi}{3\sqrt{2}N} \frac{1}{z\sqrt{h+1}} \left[3 \frac{(1-\sqrt{z})^4}{\left(1 - \frac{4}{3}\sqrt{z} + \frac{1}{2}z\right)^2} - \frac{(1-\sqrt{z})(1-3\sqrt{z})}{1 - \frac{4}{3}\sqrt{z} + \frac{1}{2}z} \right] + \mathcal{O}([h+1]^0), \quad z > 1, \\ r \stackrel{h \rightarrow -1^+}{\cong} \frac{8\pi}{3\sqrt{2}N} \frac{1}{z\sqrt{h+1}} \frac{(1-\sqrt{z})^4}{\left(1 - \frac{4}{3}\sqrt{z} + \frac{1}{2}z\right)^2} + \mathcal{O}([h+1]^0), \quad z > 1. \end{aligned} \quad (3.17)$$

In this strong coupling regime the indices become **very large** and hence in contradiction with the data. In addition, the slow roll expansion cannot be trusted when the coefficients of $1/N$ become large compared with unit. In conclusion, for $h \rightarrow -1^+$ the case of large field $z > 1$ is excluded by the data.

C. The singular limit $z = 1$ and then $h \rightarrow -1^+$ yields the Harrison-Zeldovich spectrum

We study in this section the case $z = 1$ in trinomial chaotic inflation. We obtain from eq.(3.5)

$$y \stackrel{z=1}{\cong} 1 + \frac{4}{3}h + \left(1 - \frac{4}{3}h^2\right) \log[2(1+h)] - \frac{4h}{3\Delta} \left(\frac{5}{2} - 2h^2\right) \left[\arctan\left(\frac{h+1}{\Delta}\right) - \arctan\left(\frac{h}{\Delta}\right) \right]. \quad (3.18)$$

For $z = 1$, we find from eqs.(3.6)-(3.9) and (3.18) in the limit $h \rightarrow -1^+$,

$$y \stackrel{z=1, h \rightarrow -1^+}{\cong} \frac{\pi}{3} \sqrt{\frac{1}{2(h+1)}} - \frac{1}{3} \log(h+1) + \mathcal{O}([h+1]^0),$$

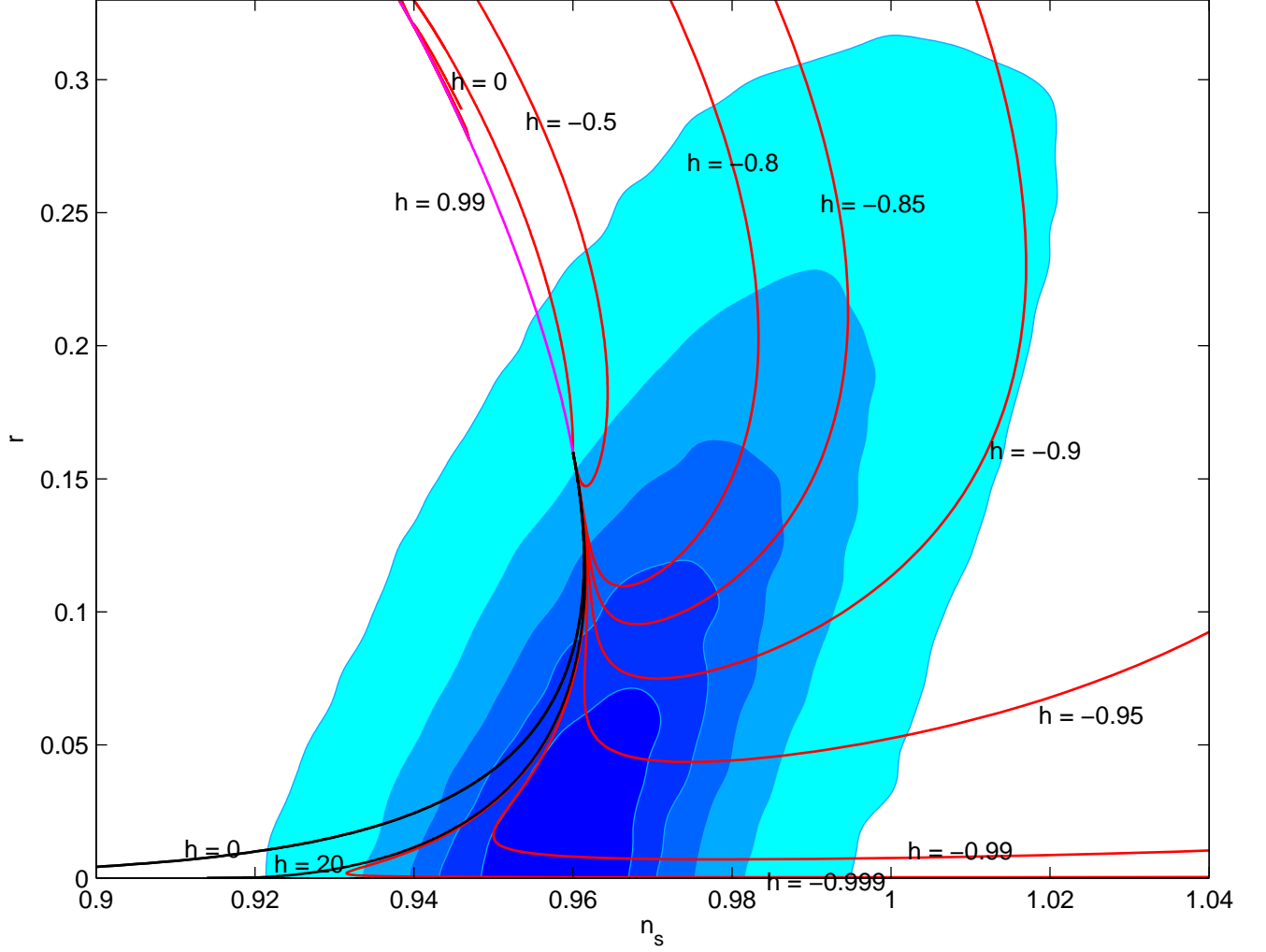


FIG. 2: Trinomial Inflation. We plot r vs. n_s for fixed values of the asymmetry parameter h and the field z varying along the curves. The red curves are those of chaotic inflation with $h \leq 0$ (only the short magenta curve has positive h), while the black curves are for new inflation. The color-filled areas correspond to 12%, 27%, 45%, 68% and 95% confidence levels according to the WMAP3 and Sloan data. The color of the areas goes from the darker to the lighter for increasing CL. New inflation only covers a narrow area between the black lines while chaotic inflation covers a much wider area but, as shown by fig. 9, this wide area is only a small corner of the field z - asymmetry h plane. Since new inflation covers the banana-shaped region between the black curves, we see from this figure that the most probable values of r are **definitely non-zero** within trinomial new inflation. Precise lower bounds for r are derived from MCMC in eq.(5.2).

$$\begin{aligned}
 n_s^{z=1, h \rightarrow -1^+} &= 1 + \frac{2\pi}{N} \sqrt{2(h+1)} [1 + \mathcal{O}(h+1)] , \\
 r^{z=1, h \rightarrow -1^+} &= \frac{16\pi}{N} \sqrt{2} (h+1)^{\frac{3}{2}} [1 + \mathcal{O}(h+1)] , \\
 |\Delta_{k ad}^{(S)}|^2 &^{z=1, h \rightarrow -1^+} = \frac{N^2}{36} \left[\frac{M}{\pi M_{Pl} (h+1)^{\frac{1}{4}}} \right]^4 .
 \end{aligned} \tag{3.19}$$

Therefore, we reach the Harrison-Zeldovich spectrum $n_s = 1$, $r = 0$ as a limiting value. This is a strong coupling regime $y \rightarrow \infty$ where in addition we must keep the ratio $M/(h+1)^{\frac{1}{4}}$ fixed for $h \rightarrow -1^+$ since it is determined by the

amplitude of the adiabatic perturbations. That is, we must keep

$$\bar{M} \equiv \frac{M}{(h+1)^{\frac{1}{4}}} \quad \text{fixed as } h \rightarrow -1^+,$$

while M as well as m go to zero. Actually, the **whole** potential $V(\phi)$ eq.(3.1) **vanishes** in this limit since,

$$\begin{aligned} m &= \frac{M^2}{M_{Pl}} \quad z=1, h \rightarrow -1^+ \quad \frac{\bar{M}^2}{M_{Pl}} \sqrt{h+1} \rightarrow 0, \\ g &= h \sqrt{\frac{y}{2N}} \left(\frac{M}{M_{Pl}}\right)^2 \quad z=1, h \rightarrow -1^+ \quad -\sqrt{\frac{\pi}{6N}} \left(\frac{\bar{M}}{M_{Pl}}\right)^2 \left(\frac{1+h}{2}\right)^{\frac{1}{4}} \rightarrow 0, \\ \lambda &= \frac{y}{8N} \left(\frac{M}{M_{Pl}}\right)^4 \quad z=1, h \rightarrow -1^+ \quad \sqrt{\frac{\pi}{24N}} \left(\frac{\bar{M}}{M_{Pl}}\right)^4 \sqrt{\frac{1+h}{2}} \rightarrow 0 \end{aligned} \quad (3.20)$$

The inflaton field is therefore a **massless** free field at $z = 1$ and $h \rightarrow -1^+$. This explains why the corresponding spectrum is the scale invariant Harrison-Zeldovich one. This is clearly a singular limit since one cannot obtain any inflation from an identically zero potential. Namely, taking the flat limit $h \rightarrow -1^+$ in the spectrum computed for $z = 1$, $h > -1$ with a fixed number of e-folds N , yields the scale invariant Harrison-Zeldovich spectrum.

Notice that here we keep the number of e-folds N *fixed* which makes the potential to vanish since otherwise the field will be stuck at the point $z = 1$ when $h = -1$ leading to eternal inflation.

In summary, this shows theoretically that the Harrison-Zeldovich spectrum is highly unplausible and unrealistic since it appears only in the singular limit $z = 1$, $h \rightarrow -1^+$ where the inflaton potential identically vanishes.

Recall that one can also get a Harrison-Zeldovich spectrum letting formally the number of e-folds N to infinity in eqs.(2.11).

D. The high asymmetry $h < -1$ regime.

In order to fulfill the finite number of e-folds condition eq.(2.9) for $h < -1$ we have to add a constant piece to the chaotic inflationary potential eq.(3.2).

We therefore consider as inflaton potential in the $h < -1$ regime,

$$w(\chi) = \frac{1}{2} \chi^2 + \frac{h}{3} \sqrt{\frac{y}{2}} \chi^3 + \frac{y}{32} \chi^4 + \frac{2}{y} G(h), \quad (3.21)$$

The absolute minimum of this potential is at

$$\chi_+ = \sqrt{\frac{8}{y}} [-h + D] \quad , \quad D \equiv \sqrt{h^2 - 1}, \quad h < -1. \quad (3.22)$$

and we have

$$\begin{aligned} G(h) &\equiv \frac{8}{3} h^4 - 4 h^2 + 1 + \frac{8}{3} |h| D^3, \\ w''(\chi_+) &= 2 \sqrt{h^2 - 1} \left(\sqrt{h^2 - 1} + |h| \right) > 0. \end{aligned} \quad (3.23)$$

That is, the inflaton mass squared in units of m^2 takes the value

$$2 D (D + |h|).$$

Here, the inflaton field rolls down the slope of the potential from its initial value larger than χ_+ till the absolute minimum of the potential at $\chi = \chi_+$.

By inserting eq.(3.21) for $w(\chi)$ into eq.(2.8) for $N[\chi]$ and setting $N[\chi] \equiv N$ we obtain the field χ or equivalently $z = \frac{y}{8} \chi^2$, at horizon exit, in terms of the coupling y and the asymmetry parameter h :

$$y = z + \frac{4}{3} h \sqrt{z} + 1 + \frac{2}{3} h (D - h) + 2 G(h) \log \frac{\sqrt{z}}{D - h} + \frac{16}{3} h (h^2 - 1) (D - h) \log \left(\frac{\sqrt{z} + h + D}{2D} \right). \quad (3.24)$$

This defines the field z as a monotonically increasing function of the coupling y for

$$0 < y < +\infty \quad , \quad z_+ = (D - h)^2 < z < +\infty .$$

Recall that χ and z corresponds to the time of horizon exit.

We obtain from eqs.(2.10), (2.11) and (3.21) the spectral index, the ratio r and the amplitude of adiabatic perturbations,

$$\begin{aligned} n_s &= 1 - \frac{y}{N} \frac{1}{(\sqrt{z} + h - D)^2} \left[\frac{6z(\sqrt{z} + h + D)^2}{[z + 2(D + \frac{h}{3})\sqrt{z} - \frac{2}{3}h(D - h) - 1]^2} - \frac{1 + 4h\sqrt{z} + 3z}{z + 2(D + \frac{h}{3})\sqrt{z} - \frac{2}{3}h(D - h) - 1} \right] , \\ r &= \frac{16y}{N} \frac{z}{(\sqrt{z} + h - D)^2} \frac{(\sqrt{z} + h + D)^2}{[z + 2(D + \frac{h}{3})\sqrt{z} - \frac{2}{3}h(D - h) - 1]^2} , \\ |\Delta_{k ad}^{(S)}|^2 &= \frac{N^2}{12\pi^2} \left(\frac{M}{M_{Pl}} \right)^4 \frac{[G(h) + 2z + \frac{8}{3}hz^{3/2} + z^2] (\sqrt{z} + h - D)^2 [z + 2(D + \frac{h}{3})\sqrt{z} - \frac{2}{3}h(D - h) - 1]^2}{y^2 z (\sqrt{z} + h + D)^2} . \end{aligned} \quad (3.25)$$

When $\sqrt{z} \rightarrow \sqrt{z_+}$, y vanishes quadratically as,

$$y \stackrel{z \rightarrow z_+}{\simeq} 2 (\sqrt{z} - \sqrt{z_+})^2 + \mathcal{O}([\sqrt{z} - \sqrt{z_+}]^3) .$$

In this limit the spectral index, the ratio r and the amplitude of adiabatic perturbations become,

$$n_s \stackrel{y \rightarrow 0}{\simeq} 1 - \frac{2}{N} \quad , \quad r \stackrel{y \rightarrow 0}{\simeq} \frac{8}{N} \quad , \quad |\Delta_{k ad}^{(S)}|^2 \stackrel{y \rightarrow 0}{\simeq} \frac{N^2}{6\pi^2} \left(\frac{M}{M_{Pl}} \right)^4 .$$

These results are **independent** of the asymmetry h and coincide with those for the purely quadratic monomial potential $\frac{1}{2}\chi^2$.

We see here that

$$\frac{8}{N} < r < \frac{16}{N} \quad , \quad 1 - \frac{3}{N} < n_s < 1 - \frac{2}{N} \quad \text{for } 0 < y < \infty . \quad (3.26)$$

Namely, the regime $h < -1$ of chaotic inflation covers values of r **larger** than the weak coupling limiting value $r = \frac{8}{N}$ eq.(3.10) and **smaller** than the $\rightarrow \infty$ pure quartic potential value $r = \frac{16}{N}$ eq.(3.12).

IV. TRINOMIAL NEW INFLATION: SPECTRAL INDEX, AMPLITUDE RATIO, RUNNING INDEX AND LIMITING CASES

We consider here new inflation described by the trinomial potential with broken symmetry investigated in ref.[8, 9]

$$V(\phi) = V_0 - \frac{m^2}{2} \phi^2 + \frac{m g}{3} \phi^3 + \frac{\lambda}{4} \phi^4 , \quad (4.1)$$

where $m^2 > 0$ and g and λ are dimensionless couplings. The corresponding dimensionless potential $w(\chi)$ takes the form

$$w(\chi) = -\frac{1}{2} \chi^2 + \frac{h}{3} \sqrt{\frac{y}{2}} \chi^3 + \frac{y}{32} \chi^4 + \frac{2}{y} F(h) , \quad (4.2)$$

where the quartic coupling y is dimensionless as well as the asymmetry parameter h . The couplings in eq.(4.1) and eq.(4.2) are related by,

$$g = h \sqrt{\frac{y}{2N}} \left(\frac{M}{M_{Pl}} \right)^2 \quad , \quad \lambda = \frac{y}{8N} \left(\frac{M}{M_{Pl}} \right)^4 , \quad (4.3)$$

and the constant w_0 [see eq.(1.4)] is related to V_0 in eq.(4.1) by

$$w_0 \equiv \frac{2}{y} F(h) = \frac{V_0}{N M^4} .$$

The constant $F(h)$ ensures that $w(\chi_+) = w'(\chi_+) = 0$ at the absolute minimum $\chi = \chi_+ = \sqrt{\frac{8}{y}}(\Delta + |h|)$ of the potential $w(\chi)$ according to eq.(2.9). Thus, inflation does not run eternally. $F(h)$ is given by

$$F(h) \equiv \frac{8}{3} h^4 + 4 h^2 + 1 + \frac{8}{3} |h| \Delta^3 \quad , \quad \Delta \equiv \sqrt{h^2 + 1} .$$

The parameter h reflects how asymmetric is the potential. Notice that $w(\chi)$ is invariant under the changes $\chi \rightarrow -\chi$, $h \rightarrow -h$. Hence, we can restrict ourselves to a given sign for h . Without loss of generality, we choose $h < 0$ and shall work with positive fields χ as in sec. III..

We have near the absolute minimum $\chi = \chi_+$,

$$w(\chi) \stackrel{\chi \rightarrow \chi_+}{\approx} \Delta(\Delta + |h|) (\chi - \chi_+)^2 + \mathcal{O}(\sqrt{y}[\chi - \chi_+]^3) \quad , \quad (4.4)$$

That is, the inflaton mass squared in units of m^2 takes the value

$$2 \Delta(\Delta + |h|) .$$

Notice that the inflaton mass squared takes the analogous value for chaotic inflation in the $h < -1$ regime changing $D \Rightarrow \Delta$ while $F(h)$ differs from $G(h)$ given by eq.(3.23) only by the sign of the $4 h^2$ term.

Recall that $y \sim \mathcal{O}(1) \sim h$ guarantees that $g \sim \mathcal{O}(10^{-6})$ and $\lambda \sim \mathcal{O}(10^{-12})$ *without* any fine tuning as stressed in ref. [7].

In fig. 3, we plot

$$\frac{y}{8(h^2 + 1)^2} w(\chi) \quad \text{as a function of} \quad \frac{\sqrt{y}}{8} \frac{\chi}{\sqrt{h^2 + 1}}$$

for several values of $h < 0$. We see that the minimum of the potential

$$\frac{\sqrt{y} \chi_+}{\sqrt{8} \sqrt{h^2 + 1}} = 1 + \frac{|h|}{\sqrt{h^2 + 1}}$$

grows as $|h|$ grows. Similarly, the maximum of the potential at the origin

$$\frac{y w(0)}{8(h^2 + 1)^2} = \frac{F(h)}{4(h^2 + 1)^2}$$

grows with $|h|$.

New inflation is obtained by choosing the initial field χ in the interval $(0, \chi_+)$. The inflaton χ slowly rolls down the slope of the potential from its initial value till the absolute minimum of the potential χ_+ .

Computing the number of e-folds from eq.(2.8), we find the field χ at horizon crossing related to the coupling y and the asymmetry parameter h . We obtain by inserting eq.(4.2) for $w(\chi)$ into eq.(2.8) and setting $N[\chi] = N$,

$$y = z - 2 h^2 - 1 - 2 |h| \Delta + \frac{4}{3} |h| (|h| + \Delta - \sqrt{z}) + \frac{16}{3} |h| (\Delta + |h|) \Delta^2 \log \left[\frac{1}{2} \left(1 + \frac{\sqrt{z} - |h|}{\Delta} \right) \right] - 2 F(h) \log [\sqrt{z} (\Delta - |h|)] \quad , \quad z \equiv \frac{y}{8} \chi^2 . \quad (4.5)$$

z turns to be a monotonically decreasing function of y : z decreases from $z = z_+ = (\Delta + |h|)^2$ till $z = 0$ when y increases from $y = 0$ till $y = \infty$. When $\sqrt{z} \rightarrow \sqrt{z_+}$, y vanishes quadratically as,

$$y \stackrel{z \rightarrow z_+}{\approx} 2 (\sqrt{z} - \sqrt{z_+})^2 + \mathcal{O}([\sqrt{z} - \sqrt{z_+}]^3) .$$

We obtain in analogous way from eqs.(2.10), (2.11) and (4.2) the spectral index, its running, the ratio r and the amplitude of adiabatic perturbations,

$$n_s = 1 - 6 \frac{y}{N} \frac{z(z + 2h\sqrt{z} - 1)^2}{[F(h) - 2z + \frac{8}{3} h z^{3/2} + z^2]^2} + \frac{y}{N} \frac{3z + 4h\sqrt{z} - 1}{F(h) - 2z + \frac{8}{3} h z^{3/2} + z^2} \quad , \quad (4.6)$$

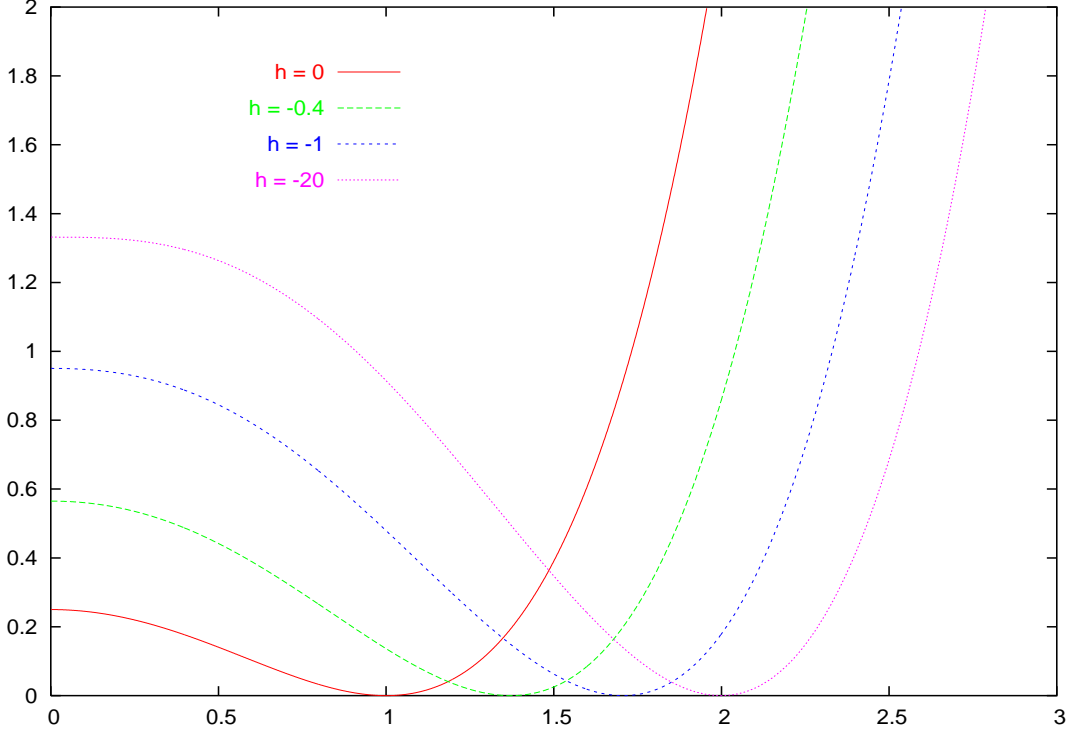


FIG. 3: Trinomial New Inflation. The new inflation trinomial potential $\frac{y w(x)}{8(h^2+1)^2}$ [eq.(4.2)] vs. the field variable $\frac{\sqrt{y} x}{\sqrt{8} \sqrt{h^2+1}}$ for different values of the asymmetry parameter $h = 0, -0.4, -1, -20$. We have normalized here the field variable and the potential by h -dependent factors in order to have a smooth $|h| \gg 1$ limit.

$$\frac{dn_s}{d \ln k} = -\frac{2}{N^2} \sqrt{z} y^2 \frac{(z + 2h\sqrt{z} - 1)(h + \frac{3}{2}\sqrt{z})}{[F(h) - 2z + \frac{8}{3}hz^{3/2} + z^2]^2} - \frac{24}{N^2} y^2 z^2 \frac{(z + 2h\sqrt{z} - 1)^4}{[F(h) - 2z + \frac{8}{3}hz^{3/2} + z^2]^4} + \frac{8}{N^2} y^2 z \frac{(3z + 4h\sqrt{z} - 1)(z + 2h\sqrt{z} - 1)^2}{[F(h) - 2z + \frac{8}{3}hz^{3/2} + z^2]^3}, \quad (4.7)$$

$$r = 16 \frac{y}{N} \frac{z(z + 2h\sqrt{z} - 1)^2}{[F(h) - 2z + \frac{8}{3}hz^{3/2} + z^2]^2}, \quad (4.8)$$

$$|\Delta_{k ad}^{(S)}|^2 = \frac{N^2}{12\pi^2} \left(\frac{M}{M_{Pl}}\right)^4 \frac{[F(h) - 2z + \frac{8}{3}hz^{3/2} + z^2]^3}{y^2 z (z + 2h\sqrt{z} - 1)^2}. \quad (4.9)$$

A. The shallow limit (weak coupling) $y \rightarrow 0$

From eq.(4.5) we see that in the shallow limit $y \rightarrow 0$, z tends to $z_+ = (\Delta + |h|)^2$. $y(z)$ has its minimum $y = 0$ at $z = z_+$. We find from eqs.(4.5)-(4.9),

$$n_s \stackrel{y \rightarrow 0}{=} 1 - \frac{2}{N} \simeq 0.96, \quad r \stackrel{y \rightarrow 0}{=} \frac{8}{N} \simeq 0.16, \quad (4.10)$$

$$\frac{dn_s}{d \ln k} \stackrel{y \rightarrow 0}{=} -\frac{2}{N^2} \simeq -0.0008, \quad |\Delta_{k ad}^{(S)}|^2 \stackrel{y \rightarrow 0}{=} \frac{N^2}{3\pi^2} \left(\frac{M}{M_{Pl}}\right)^4 \Delta(\Delta + |h|), \quad (4.11)$$

which coincide with n_s , $\frac{dn_s}{d \ln k}$ and r for the monomial quadratic potential. That is, the $y \rightarrow 0$ limit is h -independent except for $|\Delta_{k ad}^{(S)}|$. For fixed h and $y \rightarrow 0$ the inflaton potential eq.(4.2) becomes purely quadratic as we see from

eq.(4.4):

$$w(\chi) \stackrel{y \rightarrow 0}{=} \Delta(\Delta + |h|) (\chi - \chi_+)^2 + \mathcal{O}(\sqrt{y}) . \quad (4.12)$$

Notice that the amplitude of scalar adiabatic fluctuations eq.(4.10) turns out to be proportional to the square mass of the inflaton in this regime. We read this mass squared from eq.(4.12): $2 \Delta(\Delta + |h|)$ in units of m^2 . The shift of the inflaton field by χ_+ has no observable consequences. For $h = 0$ we recover the results of the monomial quadratic potential.

B. The steep limit (strong coupling) $y \rightarrow \infty$

In the steep limit $y \rightarrow \infty$, z tends to zero for new inflation. We find from eq.(4.5)

$$y \stackrel{z \rightarrow 0}{=} -F(h) \log z - q(h) - 1 + \mathcal{O}(\sqrt{z}) , \quad (4.13)$$

where

$$q(h) \equiv 2 F(h) \log(\Delta - |h|) - \frac{2}{3} (h^2 + |h| \Delta) \left\{ 8 \Delta^2 \log \left[\frac{1}{2} \left(1 - \frac{|h|}{\Delta} \right) \right] - 1 \right\} ,$$

$q(h)$ is a monotonically increasing function of the asymmetry $|h|$: $0 \leq q(h) < \infty$ for $0 < |h| < \infty$.

Then, eqs.(4.6)-(4.7) yield,

$$\begin{aligned} n_s &\stackrel{y \gg 1}{=} 1 - \frac{y}{N F(h)} , & r &\stackrel{y \gg 1}{=} \frac{16 y}{N F^2(h)} e^{-\frac{y+1+q(h)}{F(h)}} , \\ \frac{dn_s}{d \ln k} &\stackrel{y \gg 1}{=} -\frac{2 y^2 |h|}{N^2 F^2(h)} e^{-\frac{y+1+q(h)}{2 F(h)}} , \\ |\Delta_{k ad}^{(S)}|^2 &\stackrel{y \gg 1}{=} \frac{N^2}{12 \pi^2} \left(\frac{M}{M_{Pl}} \right)^4 \frac{F^3(h)}{y^2} e^{\frac{y+1+q(h)}{F(h)}} . \end{aligned} \quad (4.14)$$

In the case $h = 0$ we recover from the steep limit eqs.(4.13)-(4.14) the results for new inflation in the large y regime: we have $F(0) = 1$ and $q(0) = 0$ and eq.(4.14) becomes,

$$\begin{aligned} n_s &\stackrel{y \gg 1, h \rightarrow 0}{=} 1 - \frac{y}{N} , & r &\stackrel{y \gg 1, h \rightarrow 0}{=} \frac{16 y}{N} e^{-y-1} , \\ \frac{dn_s}{d \ln k} &\stackrel{y \gg 1, h \rightarrow 0}{=} -\frac{2 y^2 |h|}{N^2} e^{-y-1} , \\ |\Delta_{k ad}^{(S)}|^2 &\stackrel{y \gg 1, h \rightarrow 0}{=} \frac{N^2}{12 \pi^2} \left(\frac{M}{M_{Pl}} \right)^4 \frac{e^{y+1}}{y^2} . \end{aligned} \quad (4.15)$$

Notice that the slow-roll approximation is no longer valid when the coefficient of $1/N$ becomes much larger than unity.

C. The extremely asymmetric limit $|h| \rightarrow \infty$

Eqs.(4.5)-(4.9) have a finite limit for $|h| \rightarrow \infty$ with y and z scaling as h^2 . Define,

$$Z \equiv \frac{z}{h^2} , \quad Y \equiv \frac{y}{h^2} .$$

We have $0 \leq Z \leq 4$ for $+\infty \geq Y \geq 0$. Then, we find for $|h| \rightarrow \infty$ from eqs.(4.5)-(4.9) keeping Z and Y fixed,

$$\begin{aligned} Y &= Z - \frac{4}{3} \sqrt{Z} - 4 - \frac{4}{3} \log \frac{Z}{4} + \frac{16}{3 \sqrt{Z}} , \\ n_s &= 1 - 6 \frac{Y}{N} \frac{Z^2 (\sqrt{Z} - 2)^2}{\left[\frac{16}{3} - \frac{8}{3} Z^{\frac{3}{2}} + Z^2 \right]^2} + \frac{Y}{N} \frac{3 Z - 4 \sqrt{Z}}{\frac{16}{3} - \frac{8}{3} Z^{\frac{3}{2}} + Z^2} , \end{aligned} \quad (4.16)$$

$$\begin{aligned} \frac{dn_s}{d \ln k} = & -\frac{2}{N^2} Y^2 Z \frac{(\sqrt{Z}-2)(\frac{3}{2}\sqrt{Z}-1)}{[\frac{16}{3}-\frac{8}{3}Z^{3/2}+Z^2]^2} \\ & -\frac{24}{N^2} Y^2 Z^4 \frac{(\sqrt{Z}-2)^4}{[\frac{16}{3}-\frac{8}{3}Z^{3/2}+Z^2]^4} + \frac{8}{N^2} Y^2 Z^{\frac{5}{2}} \frac{(3\sqrt{Z}-4)(\sqrt{Z}-2)^2}{[\frac{16}{3}-\frac{8}{3}Z^{3/2}+Z^2]^3} \ , \end{aligned} \quad (4.17)$$

$$\begin{aligned} r = & 16 \frac{Y}{N} \frac{Z^2 (\sqrt{Z}-2)^2}{[\frac{16}{3}-\frac{8}{3}Z^{\frac{3}{2}}+Z^2]^2} \ , \\ |\Delta_{k ad}^{(S)}|^2 = & \frac{N^2 h^2}{12 \pi^2} \left(\frac{M}{M_{Pl}} \right)^4 \frac{[\frac{16}{3}-\frac{8}{3}Z^{\frac{3}{2}}+Z^2]^2}{Y^2 Z^2 (\sqrt{Z}-2)^2} \ . \end{aligned} \quad (4.18)$$

In the $|h| \rightarrow \infty$ limit, the inflaton potential takes the form

$$W(\chi) \equiv \lim_{|h| \rightarrow \infty} \frac{w(\chi)}{h^2} = \frac{32}{3Y} - \frac{1}{3} \sqrt{\frac{Y}{2}} \chi^3 + \frac{Y}{32} \chi^4 \ .$$

This is a broken symmetric potential without quadratic term. Notice that the cubic coupling has dimension of a mass in eq.(4.1) and hence this is **not** a massless potential contrary to the quartic monomial χ^4 .

In addition, eq.(4.18) shows that for large $|h|$ one must keep the product $|h| M^2$ fixed since this is determined by the amplitude of the adiabatic perturbations. We see from eq.(4.18) that in the $|h| \rightarrow \infty$ limit, $\tilde{M} \equiv \sqrt{|h|} M$ becomes the energy scale of inflation. $\tilde{M} \sim 10^{16} \text{GeV}$ [eq.(1.3)] according to the observed value of $|\Delta_{k ad}^{(S)}|/N$ displayed in eq.(2.12), while M and m vanish as $|h| \rightarrow \infty$,

$$M = \frac{\tilde{M}}{\sqrt{|h|}} \stackrel{|h| \rightarrow \infty}{=} 0 \quad , \quad m = \frac{M^2}{M_{Pl}} = \frac{\tilde{M}^2}{|h| M_{Pl}} \stackrel{|h| \rightarrow \infty}{=} 0 \quad .$$

D. Regions of n_s and r covered by New Inflation and by Chaotic Inflation.

We see from eqs.(4.7), (4.10) and (4.14) that new inflation for $h \leq 0$ covers the narrow **banana-shaped** sector between the black lines in the (n_s, r) plane depicted in fig. 2. We have in this region:

$$0 < r < \frac{8}{N} \quad , \quad n_s < 1 - \frac{1.9236 \dots}{N} \quad \text{for} \quad \infty > y > 0 \ . \quad (4.19)$$

Chaotic inflation in the $h < -1$ region covers the the even narrower **complementary** strip for $\frac{8}{N} < r < \frac{16}{N}$ eq.(3.26). The zero coupling point $y \rightarrow 0$, $r = \frac{8}{N}$, $n_s = 1 - \frac{2}{N}$ being the border between the two regimes.

Chaotic inflation for $-1 < h \leq 0$ covers a wide region depicted by the red lines in the (n_s, r) plane [see fig. 2]. However, as shown by fig. 9, this wide area is only a small corner of the field z - asymmetry h plane. Since new inflation covers the banana-shaped region between the black curves, we see from this figure that the most probable values of r are **definitely non-zero** within trinomial new inflation. Precise lower bounds for r are derived from MCMC in eq.(5.2).

V. MONTE CARLO MARKOV CHAINS AND DATA ANALYSIS WITH THE TRINOMIAL INFLATION MODELS

We performed Monte Carlo Markov Chains (MCMC) analysis of the commonly available CMB and LSS data using the CosmoMC program [12]. For CMB we considered the three years WMAP data, which provide the dominating contribution, and also small scale data (ACBAR, CBI2, BOOMERANG03). For LSS we considered SDSS (DR4). We used the second release of WMAP likelihood code. In all our MCMC runs we did not marginalize over the SZ amplitude and did not include non-linear effects in the evolution of the matter spectrum. The relative corrections are in any case not significant [6], especially in the present context.

Given a theoretical model with several free parameters and a sufficiently rich set of empirical data, MCMC is a very efficient stochastic numerical method to approximately reconstruct the probability distribution for the actual values of those parameters. It is especially useful when the theoretical predictions are themselves stochastic in nature, as is

the case of the primordial fluctuations that seed the CMB anisotropies. CosmoMC is a publicly available FORTRAN program that performs MCMC analysis over the parameter space of the Standard Cosmological model and variations thereof. The spectral index n_s of the adiabatic fluctuations and the ratio r of tensor to scalar fluctuations are two such parameters. In CosmoMC usage, one usually restrict the search to a subset of the full parameter space by imposing so-called hard constraints, whose number and type depend on previously acquired information both experimental and theoretical.

Concerning statistical convergence tests, our MCMC data were collected in parallel Message Passing Interface (MPI) runs with 10 to 16 chains, with the ‘R-1’ stopping criterion (which looks at the fluctuations among parallel chains to decide when to stop the run) set to 0.03. Typically, this meant single chains with length of the order 10^5 , with the Gelman–Rubin convergence test [$\text{var}(\text{chain mean})/\text{mean}(\text{chain var})$ in the second half of the chains] ranging from 10^{-3} to 10^{-2} for the various MCMC parameters.

We imposed as a hard constraint that r and n_s are given by the analytic expressions at order $1/N$ for the trinomial potential of the inflaton. Namely, r and n_s are given by eqs.(3.6)-(3.8) for chaotic inflation and by eqs.(4.6)-(4.8) for new inflation. Our analysis differs in this **crucial** aspect from previous MCMC studies involving the WMAP3 data [13]. As natural within inflation, we also included the inflationary consistency relation $n_T = -r/8$ on the tensor spectral index. This constraint is in any case practically negligible.

We allowed seven cosmological parameters to vary in our MCMC runs: the baryonic matter fraction ω_b , the dark matter fraction ω_c , the optical depth τ , the ratio of the (approximate) sound horizon to the angular diameter distance θ , the primordial superhorizon power in the curvature perturbation at 0.05 Mpc^{-1} , A_s , the scalar spectral index n_s and the tensor-scalar ratio r .

For comparison, we also run MCMC’s within the standard Λ CDM model augmented by the tensor-scalar ratio r (Λ CDM+ r model). That is, we treated n_s and r as unconstrained Monte Carlo parameters, using standard priors. This analysis is indeed by now quite standard and good priors are available already in CosmoMC.

We allowed the same seven parameters to vary in the MCMC runs for chaotic and new inflation.

In the case of new inflation, since the characteristic banana-shaped allowed region in the (n_s, r) plane is quite narrow and non-trivial, we used the two independent variables z and h in trinomial inflationary setup as MC parameters. That is, we used the analytic expressions at order $1/N$, eqs.(4.6) and (4.8) to express n_s and r in terms of z and h . To be more precise, rather than z we used the appropriate normalized variable

$$z_1 = 1 - \frac{z}{z_+} = 1 - \frac{z}{(\sqrt{h^2 + 1} + |h|)^2} \quad (5.1)$$

z contains the field at horizon crossing and the coupling y . z_+ stands for z at the absolute minimum of the potential. The variable z_1 grows monotonically from 0 to 1 as the coupling y grows from 0 to ∞ [see eq. (4.5) and the lines right below it].

Concerning priors, we kept the same, standard ones, of the Λ CDM+ r model for the first five parameters (ω_b , ω_c , τ , θ and A_s), while we considered all the possibilities for z_1 and h , that is $0 < z_1 < 1$, $0 < h < \infty$.

In the case of chaotic inflation we kept n_s and r as MC parameters, imposing as hard priors that they lay in the region described by chaotic inflation [see fig. 2]. This is technically convenient, since this region covers the major part of the probability support of n_s and r in the Λ CDM+ r model and the parametrization eqs.(3.6)-(3.8) in terms of the coupling parameters z and h becomes quite singular in the limit $h \rightarrow -1$. This is indeed the limit which allows to cover the region of highest likelihood.

The distributions for the field variable z and the asymmetry parameter h were obtained from the (n_s, r) distributions by a numerical change of variables using eqs.(3.6) and (3.8) and taking care of the corresponding Jacobian. We used a large collection of parallel chains with a total number of samples close to five million. In fact we did not need to explicitly compute the Jacobian. It was taken into account automatically since we used an uniform two dimensional grid in the $z-h$ plane. Quite naturally in this approach for chaotic inflation, the most likely values of the cosmological parameters and the corresponding maximum of the likelihood coincide to those of the Λ CDM+ r model.

The priors on the other parameters were the same of the Λ CDM+ r model and of new inflation.

In all our MCMC runs we keep fixed the number of e-folds N since horizon exit till the end of inflation. The reason is that the main physics that determines the value of N is **not** contained in the available data but involves the reheating era. Therefore, it is **not** reliable to fit N solely to the CMB and LSS data.

The precise value of N is certainly near $N = 50$ [16, 17]. We take here the value $N = 50$ as a reference baseline value for numerical analysis, but from the explicit expressions obtained in the slow roll $1/N$ expansion we see that both $n_s - 1$ and r scale as $1/N$.

Therefore, decreasing or increasing N produces a scale transformation in the $(n_r - 1, r)$ plane, thus displacing the black and red curves in fig. 2 towards up and left or towards down and right. This produces however small quantitative changes in our bounds for r as well as in the most probable values for r and n_s . We ran MCMC simulations with variable N and imposing the trinomial new inflation potential. As a result, we found that $N \sim 50$ was the most probable value. A sharp fall in the likelihood happens for $N < 50$ and a significant decrease shows up for $N > 50$. In summary, varying N has no dramatic effects and $N \sim 50$ turns to be the most probable value. The detailed analysis with variable N is beyond the scope of the present paper.

We have not introduced the running of the spectral index $dn_s/d \ln k$ in our MCMC fits since the running [eq. (2.11)] must be very small of the order $\mathcal{O}(N^{-2}) \sim 0.001$ in slow-roll and for generic potentials [7]. Indeed we found that adding $dn_s/d \ln k$, as given by eq. (3.7) or eq. (4.7), to the MCMC analysis yields insignificant changes on the fit of n_s and r .

On the contrary, when the running is introduced as a free parameter, then the fit of n_s and r gets worse and values for the running much larger than $\mathcal{O}(N^{-2}) \sim 0.001$ follow [6, 13]. We think that the present data are **not** yet precise enough to allow a determination of $dn_s/d \ln k$. That is, adding further parameters to the fit (like the running) does not improve the fit and does not teach anything new.

A. MCMC results for new inflation.

Our results for the new inflation trinomial potential eq.(4.2) are summarized in figs. 4 and 6.

In fig. 4 we plot the marginalized probability distributions (normalized to have maximum equal to one) of the most relevant cosmological parameters, which are the primary ones allowed to vary independently in the MCMC runs and some derived ones. The solid blue curves refer to the runs with the hard priors specific of trinomial new inflation. The dashed red curves are those of the Λ CDM+ r model. As should have been expected from fig. 2, the really significant changes are restricted solely to n_s and r . To provide further evidence of this, we compare in fig. 5 the joint probability (τ, n_s) and (τ, r) distributions of trinomial new inflation with those of the Λ CDM+ r model. We recall that the optical depth parameter τ is strongly correlated with n_s .

In the lower panels of fig. 6 we provide an enlarged version of the marginalized probability distributions for n_s and r , together with their mean likelihoods.

Notice the difference between probability distributions and mean likelihood distributions in the first four panels of both figs. 6 and 8. Probability and mean likelihood depend quite differently on the shapes and parametrizations of the allowed regions; if observational data were well concentrated within the allowed regions, both types of distributions would have a gaussian-like shape and the difference would be much smaller. With the current data, the joint probability distributions over the parameters of the trinomial potential are very far from gaussian, as can be appreciated from fig. 9.

The theoretical constraints narrow the allowed region of parameters in a very nontrivial way. Otherwise, the parameters could cover a much wider region. Hence, the theoretically constrained distributions can hardly be and in fact are not gaussian. In the case of trinomial new inflation, the narrow banana-shaped region depicted in fig. 2 is responsible for the marked difference between marginalized probability distribution and mean likelihood for n_s , as shown in fig. 6. Besides, the banana-shape of trinomial new inflation in the $n_s - r$ plane, produces a spike in the left lower panel of fig. 6. The sharp cut on the right is due to the theoretical upper bound on n_s given by eq. (4.19), the sharp rise on the left of the maximum is due to the marginalization over r .

We find a **lower bound** on r for the trinomial new inflation model:

$$r > 0.016 \quad (95\% \text{ CL}) \quad , \quad r > 0.049 \quad (68\% \text{ CL}) \quad (\text{new inflation}) . \quad (5.2)$$

For n_s we find:

$$n_s > 0.945 \quad (95\% \text{ CL}) \quad (\text{new inflation}) .$$

The most likely values, which can be read off directly from MCMC data, are

$$n_s \simeq 0.956 \quad , \quad r \simeq 0.055 \quad (\text{new inflation}) .$$

The results for $\max(-\log(\text{likelihood}))$ are as follows:

Λ CDM+ r model : 2714.038

Trinomial chaotic inflation : 2714.038 and Trinomial new inflation: 2714.153

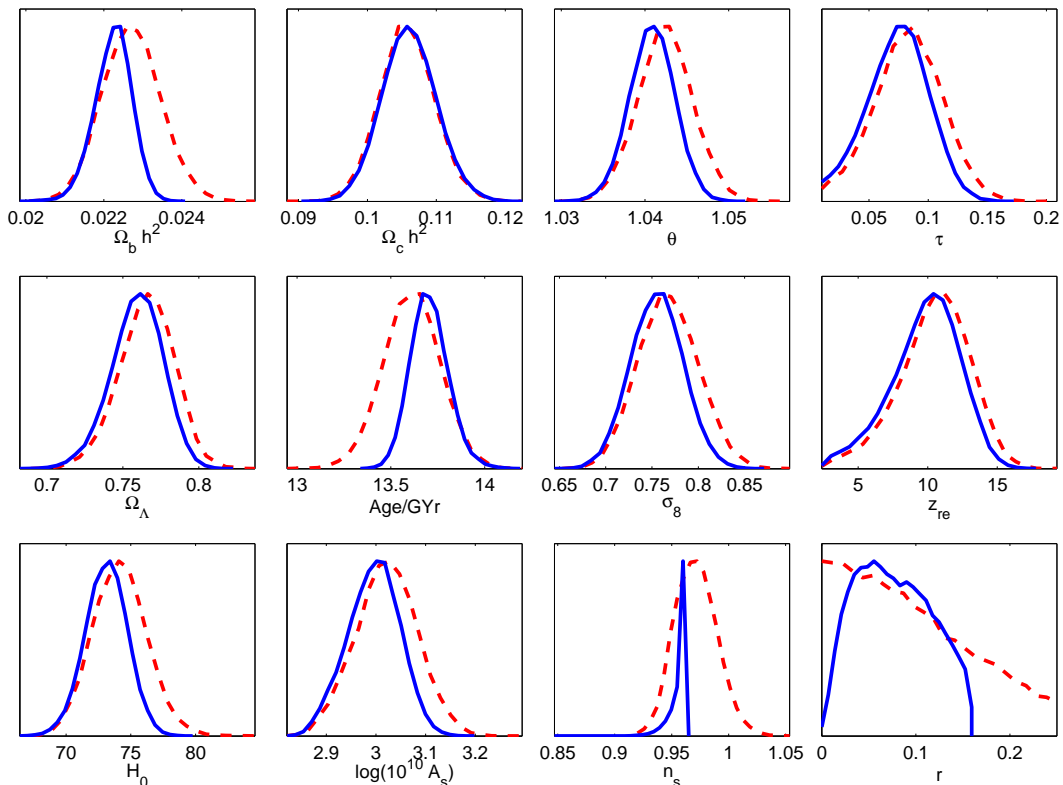


FIG. 4: Comparison of the marginalized probability distributions (normalized to have maximum equal to one) of the most relevant cosmological parameters (both primary and derived) between Trinomial New Inflation (solid blue curves) and the Λ CDM+ r model (dashed red curves).

At the point with most likely values for the cosmological parameters we see a small increase of 0.115 of $-\log(\text{likelihood})$ for new inflation with respect to the Λ CDM+ r model. This increase is only twice as much of the standard deviation of $\max(-\log(\text{likelihood}))$ over ten parallel chains, which is 0.062 in the case of the Λ CDM+ r model. Therefore, this increase of the $-\log(\text{likelihood})$ for new inflation is not significant.

We recall that for trinomial new inflation there exist the theoretical upper limits: $n_s \leq 0.9615\dots$, $r \leq 0.16$ [9]. That is, the *most probable* value of n_s for trinomial new inflation is very close to its *theoretical limiting* value and that of r is not too far from it (see also fig. 6).

In the upper panels of fig. 6 we plot the marginalized probabilities and the mean likelihoods for the normalized coupling at horizon exit z_1 and for y and h , that is the two parameters of the trinomial potential of new inflation. Their most likely values in our MCMC runs,

$$z_1 \simeq 0.886, \quad y \simeq 2.01 \quad \text{and} \quad h \simeq 0.266 \quad (\text{new inflation}),$$

are not extremely significant in view of the shapes of probabilities and mean likelihoods in fig. 6. More appropriate quantifiers are the upper bounds

$$y < 2.46, \quad h < 1.2 \quad \text{with 68\% CL}, \quad y < 6.35, \quad h < 4.92 \quad \text{with 95\% CL} \quad (\text{new inflation}) \quad (5.3)$$

The z_1 distribution decreases for small z_1 (that is, where one approaches the quadratic monomial potential at $y = 0$) because such case yields a too large value for r , ($r \rightarrow 0.16$) with respect to the experimental data. For $\tilde{z} \rightarrow 1$ the \tilde{z} distribution decreases too because in this case one gets a too small spectral index n_s .

In conclusion, the most likely trinomial potentials for new inflation are almost symmetric and have moderate nonlinearity with the quartic coupling y of order 1. The $\chi \rightarrow -\chi$ symmetry is here broken since the absolute minimum of the potential is at $\chi \neq 0$.

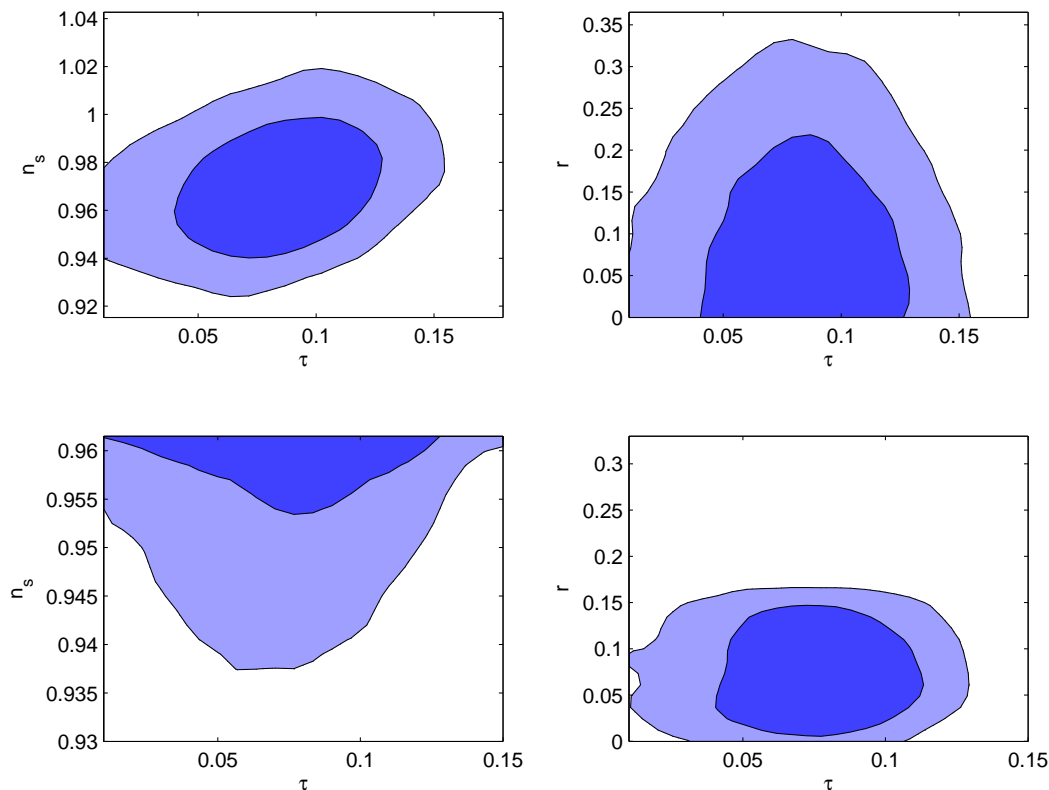


FIG. 5: Upper panels: 95% and 68% percent contour plots of joint probability (τ, n_s) distribution (left) and (τ, r) distribution (right) in the $\Lambda\text{CDM}+r$ model. Lower panels: the two joint distributions in trinomial new inflation. Recall that in this case $n_s < 0.9615\dots$ is a theoretical bound when $N = 50$.

B. MCMC results for chaotic inflation.

Our results for the trinomial potential of chaotic inflation, eq.(4.2), are summarized in figs. 7, 8 and 9.

In fig. 7 we plot the marginalized probability distributions (normalized to have maximum equal to one) of the usual cosmological parameters as in fig. 4. Again, solid blue curves refer to the runs with the hard priors of chaotic inflation, while the dashed red curves are those of the $\Lambda\text{CDM}+r$ model. As should have been expected from fig. 2, there are no really significant changes in any parameter.

In the upper panels of fig. 8 we plot the marginalized probabilities and the mean likelihoods for the parameters of the trinomial potential of chaotic inflation, the normalized coupling at horizon exit z , the quartic coupling y and the asymmetry h . These are numerically calculated from those of n_s and r (which are also reported in the lower panels of fig. 8), by means of eqs. (3.6), (3.8) and (3.24). The strong non-linearities of these relations are responsible for the peculiar shapes of the probabilities and mean likelihoods, and their marked relative differences, of the variables in the upper panels.

Finally, in fig. 9 we depict the confidence levels at 12%, 27%, 45%, 68% and 95% in the (z, h) plane. The chaotic symmetric trinomial potential $h = 0$ is almost certainly **ruled out** since $h < -0.7$ at 95 % confidence level.

We see that the maximum probability is for strong asymmetry $h \lesssim -0.9$ and significant nonlinearity $0.5 \lesssim z \lesssim 1$ and $2.5 \lesssim y \lesssim 5$. That is, *all three* terms in the trinomial potential $w(\chi)$ *do contribute to the same order*.

Notice that the range $0.5 < z < 1$ corresponds for $h \rightarrow -1^+$ to the region where the quartic coupling is quite significant: $4.207\dots < y < +\infty$ according to eq.(3.13).

The probability is maximum on a highly special and narrow corner in the (z, h) parameter space. This suggests:

- (i) the data force both the asymmetry as well as the coupling to be **large**.
- (ii) the fact that $z \sim 1$ implies large y means that we are in the nonlinear regime in z , that is strong coupling in χ . This suggests that higher order terms may be added and will be relevant.
- (iii) If the preferred values are near the boundary of the parameter space, it could be that the true potential is **beyond** that boundary. The region of parameter space in which trinomial chaotic inflation yields $r \ll 1$ is

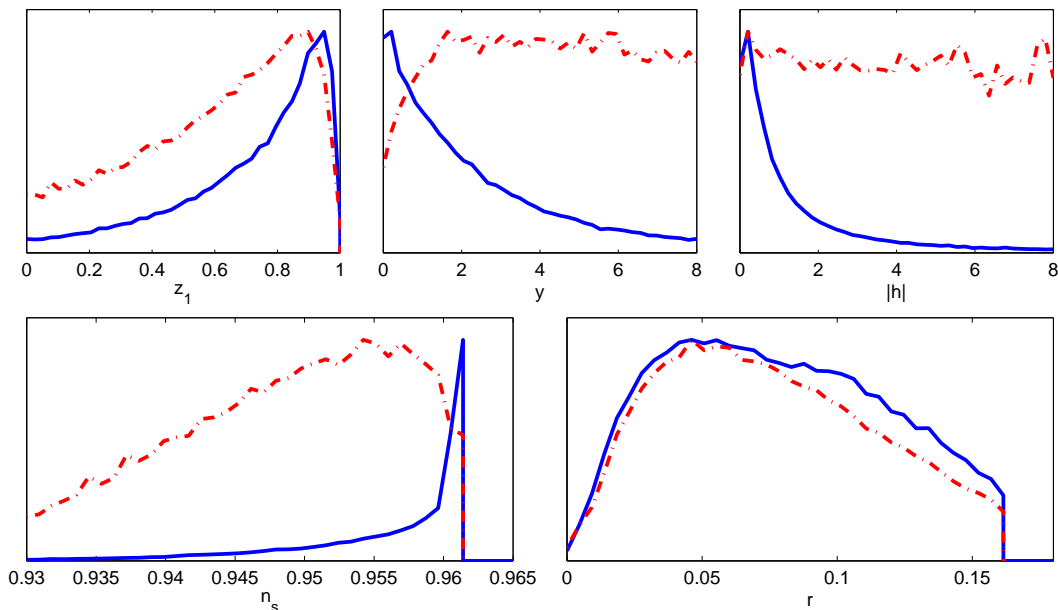


FIG. 6: Trinomial New Inflation. Upper panels: probability distributions (solid blue curves) and mean likelihoods (dot-dashed red curves), all normalized to have maximum equal to one, for the values of the normalized coupling at horizon exit z_1 , of the quartic coupling y and of the modulus $|h|$ of the asymmetry of the potential. Lower panels: probabilities and mean likelihoods for the values of n_s and r . Notice that here $n_s < 0.9615\dots$ and $r \leq 0.16$ since these are the theoretical upper bounds for n_s and r in trinomial new inflation with $N = 50$. Trinomial new inflation exhibits a **lower bound** for the ratio: $r > 0.016$ (95% CL), $r > 0.049$ (68% CL).

very narrow and highly non-generic and corresponds to an inflaton potential contrary to the Landau-Ginsburg spirit since adding higher degree terms in the field to the trinomial potential can produce relevant changes. This means that the fit for chaotic inflation can be unstable while for new inflation the maximum probability happens for a moderate nonlinearity and therefore will not be much affected by higher degree monomials. Finally, the $r \rightarrow 0$ regime is obtained near the singular point $z = 1$, $h = -1$ where the inflaton potential vanishes.

- (iv) The MCMC runs appear to go towards the $h = -1$ limiting chaotic potential exhibiting an inflexion point [see fig. 1] which is at the boundary of the space of parameters. This may indicate that the true potential is **not** within the class of chaotic potentials. Since the runs go towards the maximal value of the asymmetry parameter h where the inflaton potential exhibits an inflexion point, this supports the idea that the true potential **must** definitely break the $\chi \rightarrow -\chi$ symmetry, as new inflaton potentials do spontaneously. This favours again new inflation since the best fit to the trinomial new inflation potential corresponds to small or zero asymmetry parameter h . The spontaneous breakdown of the symmetry seems enough to obtain the best fit to the data without the presence of an explicit symmetry breaking term $\frac{h}{3} \sqrt{\frac{y}{2}} \chi^3$ [see eq.(4.2)].

C. Conclusions.

The MCMC results for chaotic and new inflation presented above show that:

- (i) symmetry breaking is begged by the data. Namely, in chaotic inflation the data ask for a strongly asymmetric potential since we find the maximum probability when h is near the extreme value $h = -1$. In chaotic inflation, the $h = 0$ case is almost certainly ruled out as noticed above. In new inflation the symmetry is spontaneously broken by construction since the absolute minima is at $\chi \neq 0$. Hence, in one way or the other the data **request** a breakdown either explicit or spontaneous of the $\chi \rightarrow -\chi$ symmetry.

New inflation naturally satisfies this requirement since the spontaneous symmetry breaking can alone reproduce the data with a moderate nonlinearity.

- (ii) Adding higher order terms to the trinomial new inflation potential will not affect the trinomial fit since it corresponds to a moderate nonlinearity $z_1 = 0.886$. On the contrary, adding higher order terms in trinomial

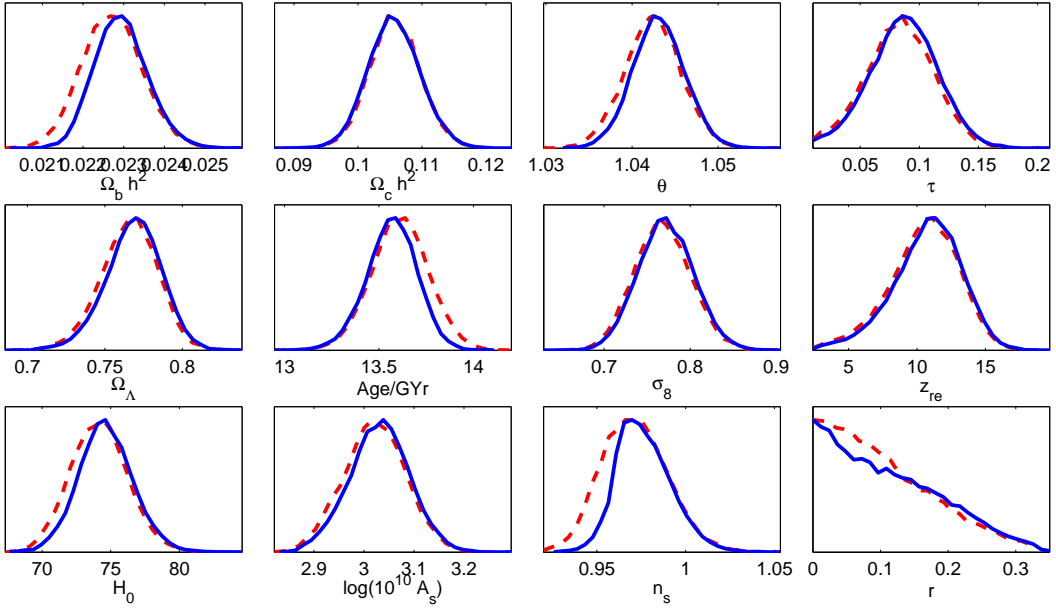


FIG. 7: Comparison of the marginalized probability distributions (normalized to have maximum equal to one) of the most relevant cosmological parameters (both primary and derived) between Trinomial Chaotic Inflation (solid blue curves) and the Λ CDM+ r model (dashed red curves).

chaotic inflation can change the trinomial fit since we find a significant nonlinearity $0.5 < z < 1$ with the trinomial chaotic potential. Therefore, in chaotic inflation, each time a new term of higher degree is added to the potential, it changes significantly all the coefficients in the potential. This is against the Landau-Ginsburg spirit which is the framework of the effective theory of inflation.]

- (iii) Inflaton potentials of degree higher than four have been recently investigated in ref. [15]. It is shown in ref. [15] that binomial potentials with quadratic and χ^{2n} terms reproduce the data in domains which are larger for $n = 2$ than for $n > 2$. In addition, for new inflation it is shown that the crucial region to reproduce the data is the neighbourhood of the absolute minima of the potential. That is, only the quadratic and somehow the quartic terms around χ_+ are relevant to fit the data.

In summary, the MCMC analysis of the CMB+LSS data indicates that new trinomial inflation is the best model.

Trinomial new inflation gives a very good fit to the data (CMB+LSS) with a moderate nonlinearity and small or zero asymmetry parameter. That is, the potential which best fits the data is the spontaneously broken symmetry potential eq.(4.2) with $h = 0$ and $y \simeq 2.01 \dots$

$$w(\chi) = \frac{y}{32} \left(\chi^2 - \frac{8}{y} \right)^2,$$

Moreover, we have for this potential, when $N = 50$,

$$n_s \simeq 0.956 \quad , \quad r \simeq 0.055 \quad (\text{new inflation}).$$

- (iv) More generally, we have a **lower bound** on the ratio r within the trinomial new inflationary potentials given by

$$r > 0.016 \text{ (95\% CL)}, \quad r > 0.049 \text{ (68\% CL)} \quad (\text{new inflation}).$$

Acknowledgment: The Monte Carlo simulations were performed at the Avogadro-Golgi clusters at CILEA and on the Atena cluster at Dipartimento di Fisica, Università Milano-Bicocca.

[1] D. Kazanas, ApJ 241, L59 (1980); A. H. Guth, Phys. Rev. **D23**, 347 (1981); K. Sato, MNRAS, **195**, 467 (1981).

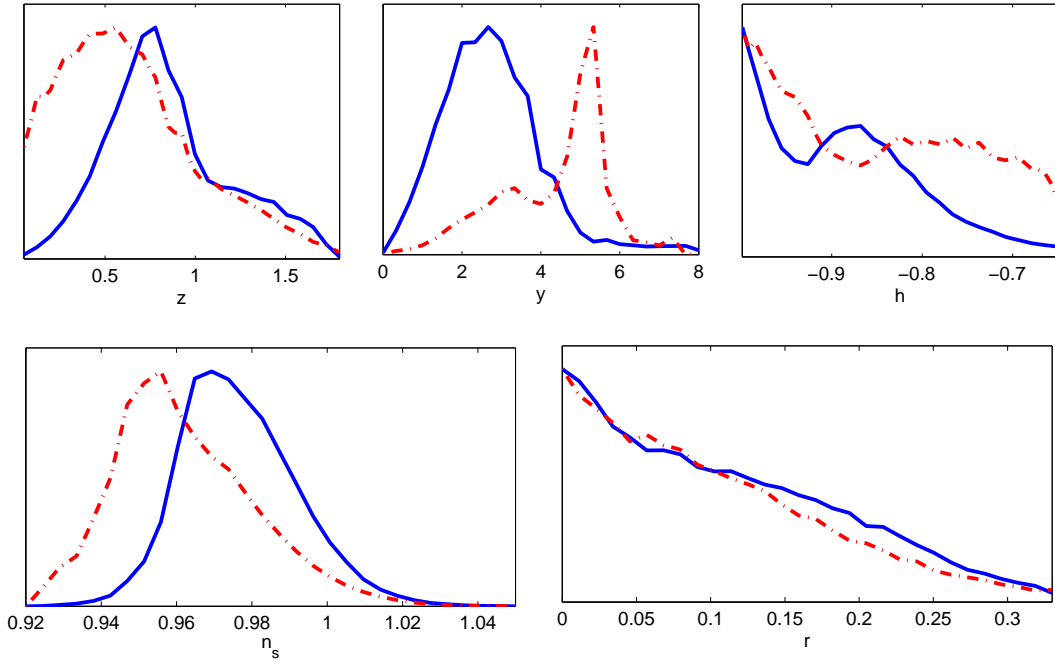


FIG. 8: Trinomial Chaotic Inflation. Upper panels: probability distributions (solid blue curves) and mean likelihoods (dashed red curves), all normalized to have maximum equal to one, for the values of the normalized coupling at horizon exit z , of the quartic coupling y and of the asymmetry h of the potential. Lower panels: probabilities and mean likelihoods for the values of n_s and r . The data request a strongly asymmetric potential in chaotic inflation. That is, a strong breakdown of the $\chi \rightarrow -\chi$ symmetry.

- [2] V. F. Mukhanov , G. V. Chibisov, Soviet Phys. JETP Lett. **33**, 532 (1981). S. W. Hawking, Phys. Lett. **B115**, 295 (1982). A. H. Guth , S. Y. Pi, Phys. Rev. Lett. **49**, 1110 (1982). A. A. Starobinsky, Phys. Lett. **B117**, 175 (1982). J. M. Bardeen, P. J. Steinhardt , M. S. Turner, Phys. Rev. **D28**, 679 (1983). V. F. Mukhanov, H. A. Feldman , R. H. Brandenberger, Phys. Rept. **215**, 203 (1992).
- [3] P. Coles and F. Lucchin, *Cosmology*, John Wiley, Chichester, 1995. A. R. Liddle and D. H. Lyth, *Cosmological Inflation and Large Scale Structure*, Cambridge University Press, 2000. S. Dodelson, *Modern Cosmology*, Academic Press, 2003. D. H. Lyth , A. Riotto, Phys. Rept. **314**, 1 (1999).
- [4] M. S. Turner, Phys. Rev. **D48**, 3502 (1993). A. R. Liddle, P. Parsons , J. D. Barrow, Phys. Rev. **D50**, 7222 (1994). S. Dodelson, W. H. Kinney, E. W. Kolb, Phys. Rev. **D56**, 3207 (1997). W. Hu and S. Dodelson, Ann. Rev. Astron. Ap. **40**, 171 (2002); J. Lidsey, A. Liddle, E. Kolb, E. Copeland, T. Barreiro and M. Abney, Rev. of Mod. Phys. **69**, 373, (1997). W. Hu, astro-ph/0402060. S. M. Leach, A. R. Liddle, J. Martin, D. J. Schwarz, Phys. Rev. **D66**, 023515 (2002). N. Bartolo, S. Matarrese, A. Riotto, Phys. Rev. **D64**, 083514 (2001). N. Bartolo, E. Komatsu, S. Matarrese, A. Riotto, Phys. Rept. **402** (2004) 103. S. M. Leach, A. R. Liddle, Phys. Rev. **D68**, 123508 (2003). V. Barger, H. S. Lee, D. Marfatia, Phys. Lett. **B565**, 33 (2003). K. Kadota, S. Dodelson, W. Hu, E. D. Stewart, Phys. Rev. **D72** (2005) 023510
- [5] C. L. Bennett *et.al.* (WMAP collaboration), Ap. J. Suppl. **148**, 1 (2003). A. Kogut *et.al.* (WMAP collaboration), Ap. J. Suppl. **148**, 161 (2003). D. N. Spergel *et. al.* (WMAP collaboration), Ap. J. Suppl. **148**, 175 (2003). H. V. Peiris *et.al.* (WMAP collaboration), Ap. J. Suppl. **148**, 213 (2003).
- [6] D. N. Spergel *et. al.* (WMAP collaboration), astro-ph/0603449. L. Page, *et. al.* (WMAP collaboration), astro-ph/0603450. G. Hinshaw, *et. al.* (WMAP collaboration), astro-ph/0603451. N. Jarosik, *et. al.* (WMAP collaboration), astro-ph/0603452.
- [7] D. Boyanovsky, H. J. de Vega, N. G. Sánchez, Phys. Rev. **D 73**, 023008 (2006).
- [8] D. Cirigliano, H. J. de Vega, N. G. Sanchez, Phys. Rev. **D 71**, 103518 (2005).
- [9] H. J. de Vega, N. G. Sanchez, Phys. Rev. **D 74**, 063519 (2006).
- [10] L. D. Landau, E. M. Lifshits, ‘Physique Statistique’, chapter 14, Mir Ellipses, Paris, 1994. H. Leutwyler, Ann. Phys. **235**, 165 (1994), hep-ph/9409423. S. Weinberg, hep-ph/9412326 and ‘The Quantum Theory of Fields’, vol. 2, Cambridge University Press, Cambridge, 2000.
- [11] See the SDSS home page <http://www.sdss.org/>. M. Tegmark et al. [SDSS Collaboration], Astrophys. J. **606**, 702 (2004). D.J. Eisenstein et al, Astrophys. J. **633**, 560 (2005). M. Tegmark, D. Eisenstein, M. Strauss et al, Phys. Rev. **D74**, 123507

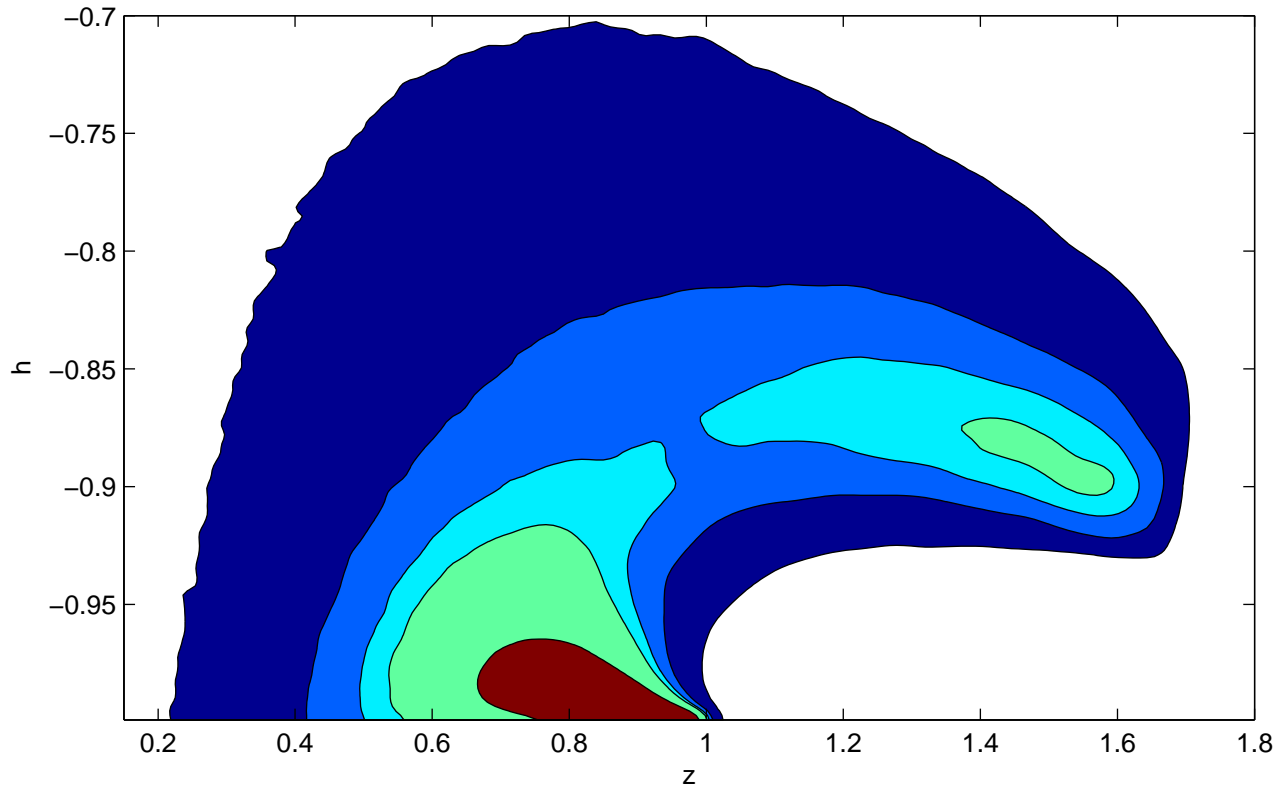


FIG. 9: Trinomial Chaotic Inflation. 12%, 27%, 45%, 68% and 95% confidence levels of the probability distribution in the field z - asymmetry h plane. The color of the areas goes from brown to dark blue for increasing CL. We see a strong preference for a very asymmetric potential with $h < -0.95$ and a significant nonlinearity $0.7 < z < 1$ in chaotic inflation.

(2006).

- [12] A. Lewis, S. Bridle, Phys. Rev. D66, 103511 (2002). <http://cosmologist.info/cosmomc/>
- [13] H. Peiris, R. Easther, JCAP 0607, 002 and 0610, 017, (2006). F. Finelli, M. Rianna, N. Mandolesi, JCAP 0612 (2006) 006. A. R. Liddle et al., Phys. Rev. D 74, 083512 (2006). K. M. Huffenberger, H. K. Eriksen, F. K. Hansen, Astrophys. J. 651, L81 (2006). H. K. Eriksen et al., ApJ, 656, 641 (2007). D. Parkinson, P. Mukherjee, A. R. Liddle, Phys. Rev. D73 (2006) 123523. M. Viel, M. G. Haehnelt, A. Lewis, Mon. Not. Roy. Astron. Soc. Lett. 370 (2006) L51. B. Feng, J. Q. Xia, J. Yokoyama, astro-ph/0608365. M. Bridges, A.N. Lasenby, M.P. Hobson, MNRAS, 369, 1123 (2006). Y. Wang, P. Mukherjee, Astrophys. J. 650 (2006) 1.
- [14] M. B. Hoffman, M. S. Turner, Phys. Rev. D64, 023506 (2001), W. H. Kinney, Phys. Rev. D66, 083508 (2002), R. Easther, W. H. Kinney, Phys. Rev. D67, 043511 (2003). L. A. Boyle, P. J. Steinhardt, N. Turok, Phys. Rev. Lett. 96 (2006) 111301. W. H. Kinney, arXiv:0706.3699; B. A. Powel, W. H. Kinney, arXiv:0706.1982. W. H. Kinney, E. W. Kolb, A. Melchiorri, A. Riotto, Phys. Rev. D74 (2006) 023502. C. Y. Chen et al., Class. Quant. Grav. 21, 3223 (2004). E. Ramirez, A. R. Liddle, Phys. Rev. D71, 123510 (2005). R. Easther, J. T. Giblin, Phys. Rev. D72, 103505 (2005). S. Chongchitnan, G. Efstathiou, Phys. Rev. D72, 083520 (2005). M. Spalinski, arXiv:0706.2503.
- [15] D. Boyanovsky, H. J. de Vega, C. M. Ho, N. G. Sánchez, Phys. Rev. **D75**, 123504 (2007).
- [16] E. W. Kolb and M. S. Turner, *The Early Universe* Addison Wesley, Redwood City, C.A. 1990. S. Dodelson, *Modern Cosmology*, Academic Press, 2003.
- [17] W. H. Kinney, A. Riotto, JCAP **0603**, 0.11 (2006); M. Giovannini, arXiv:astro-ph/0703730.